Cellular/Molecular

Tonic Activation of NR2D-Containing NMDARs Exacerbates Dopaminergic Neuronal Loss in MPTP-Injected Parkinsonian Mice

Ramesh Sharma,[1,2,3] Chiranjivi Neupane,[1,2,3] Thuy Linh Pham,[1,2] Miae Lee,[2] Sanghoon Lee,[3] So Yeong Lee,[3] Min-Ho Nam,[4] Cuk-Seong Kim,[1,2] and Jin Bong Park[3]

[1]Department of Biomedicine, Chungnam National University, Daejeon 35015, Republic of Korea, [2]Physiology, Chungnam National University, Daejeon 35015, Republic of Korea, [3]Laboratory of Veterinary Pharmacology, College of Veterinary Medicine and Research Institute for Veterinary Science, Seoul National University, Seoul 08852, Republic of Korea, and [4]Brain Science Institute, Korea Institute of Science and Technology (KIST), Seoul 02792, Republic of Korea

NR2D subunit-containing NMDA receptors (NMDARs) gradually disappear during brain maturation but can be recruited by pathophysiological stimuli in the adult brain. Here, we report that 1-methyl-4-phenyl-1,2,3,6-tetrahydropyridine (MPTP) intoxication recruited NR2D subunit-containing NMDARs that generated an Mg^{2+}-resistant tonic NMDA current (I_{NMDA}) in dopaminergic (DA) neurons in the midbrain of mature male mice. MPTP selectively generated an Mg^{2+}-resistant tonic I_{NMDA} in DA neurons in the substantia nigra pars compacta (SNpc) and ventral tegmental area (VTA). Consistently, MPTP increased NR2D but not NR2B expression in the midbrain regions. Pharmacological or genetic NR2D interventions abolished the generation of Mg^{2+}-resistant tonic I_{NMDA} in SNpc DA neurons, and thus attenuated subsequent DA neuronal loss and gait deficits in MPTP-treated mice. These results show that extrasynaptic NR2D recruitment generates Mg^{2+}-resistant tonic I_{NMDA} and exacerbates DA neuronal loss, thus contributing to MPTP-induced Parkinsonism. The state-dependent NR2D recruitment could be a novel therapeutic target for mitigating cell type-specific neuronal death in neurodegenerative diseases.

Key words: **dopaminergic neurons; MPTP; NR2D; SNpc; tonic NMDA**

Significance Statement

NR2D subunit-containing NMDA receptors (NMDARs) are widely expressed in the brain during late embryonic and early postnatal development, and then downregulated during brain maturation and preserved at low levels in a few regions of the adult brain. Certain stimuli can recruit NR2D subunits to generate tonic persistent NMDAR currents in nondepolarized neurons in the mature brain. Our results show that MPTP intoxication recruits NR2D subunits in midbrain dopaminergic (DA) neurons, which leads to tonic NMDAR current-promoting dopaminergic neuronal death and consequent abnormal gait behavior in the MPTP mouse model of Parkinson's disease (PD). This is the first study to indicate that extrasynaptic NR2D recruitment could be a target for preventing neuronal death in neurodegenerative diseases.

Introduction

NMDA receptors (NMDARs) are the most abundant ligand-gated ion channels in the brain. Their main function is to regulate physiological synaptic plasticity in excitatory synapses. In addition to playing a physiological role in developmental plasticity, learning, and memory, pathological over-excitation of NMDARs has been linked to neuronal damage in various neurologic diseases. NMDARs are tetrameric assemblies including at least one of four different NR2 subunits (A, B, C, and D). NR2D subunit-containing NMDARs are exclusively extrasynaptic in some brain regions (Lozovaya et al., 2004; Paoletti et al., 2013). In general, the pathological activation of extrasynaptic NMDARs (eNMDARs) plays a major role in triggering apoptotic pathways in various brain diseases (Hardingham and

Received Oct. 17, 2022; revised Sep. 1, 2023; accepted Sep. 8, 2023.

Author contributions: R.S., C.N., T.L.P., M.L., S.L., S.Y.L., M.-H.N., C.-S.K., and J.B.P. designed research; R.S. and C.N. performed research; R.S., C.N., and J.B.P. analyzed data; R.S. wrote the first draft of the paper; M.-H.N. edited the paper; J.B.P. wrote the paper.

This work was supported by National Research Foundation of Korea (NRF) Grants 2021R1I1A3051864 and 2023R1A2C100524811 and the New Faculty Startup Fund from Seoul National University Grant 550-20220057.

C. Neupane's present address: Department of Physiology, David Geffen School of Medicine, University of California, Los Angeles, Los Angeles, California 90095-1751.

T. L. Pham's present address: Department of Histopathology, Hai Phong University of Medicine & Pharmacy, Hai Phong 042-12, Vietnam.

The authors declare no competing financial interests.

Correspondence should be addressed to Jin Bong Park at jbpark@snu.ac.kr.

https://doi.org/10.1523/JNEUROSCI.1955-22.2023

Bading, 2010; S.J. Zhang et al., 2011; Kaufman et al., 2012; Milnerwood et al., 2012). By contrast, the classical synaptic counterparts tend to stimulate multiple pro-survival pathways, leading to neuroprotective effects (Y. Liu et al., 2007; Hardingham and Bading, 2010; Stark and Bazan, 2011; Kaufman et al., 2012). Thus, eNMDARs containing the NR2D subunit may contribute to neuronal excitotoxicity. While NR2D is widely expressed during late embryonic and early postnatal development, it is generally preserved at low levels only in a few regions of the mature brain (Watanabe et al., 1992; Monyer et al., 1994; Dunah et al., 1996; Wenzel et al., 1996; Q. Liu and Wong-Riley, 2010). Thus, the pathophysiology of NR2D-containing eNMDARs underlying excitotoxic neuronal damage remains elusive in the adult brain.

In a recent study, pathophysiological osmotic stimulation recruited NR2D-containing eNMDARs in the adult brain, which generated Mg^{2+}-resistant tonic NMDAR currents (I_{NMDA}) in magnocellular neuroendocrine cells (MNCs) (Neupane et al., 2021). Mg^{2+}-resistant tonic I_{NMDA} satisfied the biochemical properties of NR2D-containing eNMDARs in terms of the ability to sense ambient glutamate in extrasynaptic sites. However, during osmotic stimulation, it contributed to an increase in the neuronal excitability of MNCs that secrete antidiuretic hormones, rather than to excitotoxic neuronal damage. Thus, whether pathologic recruitment of extrasynaptic NR2D is a component of neuronal loss in the adult brain has yet to be established.

The invariable loss of dopaminergic (DA) neurons in the substantia nigra pars compacta (SNpc) is the cardinal neuroanatomical feature of Parkinson's disease (PD), which is the second most common neurodegenerative disease (Bissonette and Roesch, 2016). In SNpc DA neurons, the single-channel properties of NMDARs (Jones and Gibb, 2005) and the sensitivity of evoked EPSCs in response to PPDA, which is an NR2D antagonist, are in agreement with neuronal NR2D protein expression (Dunah et al., 1996). However, the pathophysiology of NR2D-containing NMDARs has not been characterized in terms of the properties of eNMDARs in PD. In this study, we demonstrated that the recruitment of homodimeric NR2D subunit-containing eNMDARs generated Mg^{2+}-resistant tonic I_{NMDA} in SNpc DA neurons. We further suggest that neuronal death in MPTP-injected PD mice is depend on the presence of relatively high neuronal current densities.

Materials and Methods

Animals and dugs treatment

All animal experiments were approved by the Chungnam National University Institutional Animal Care and Use Committee (registration no. 202103A-CNU-043) and conducted in accordance with the National Institute of Health Guide for the Care and Use for Laboratory Animals. Equal numbers of six-week-old male wild-type (WT) and NR2D knockout (KO) C57BL/6N mice weighing 20–24 g were randomly assigned to 100-µl saline injection (control; CTL) and 1-methyl- 4-phenyl-1, 2, 3, 6-tetrahydropyridine (MPTP) injection groups. MPTP (30 mg/kg, i.p.; BID) was injected for 5 consecutive days. MPTP use and safety precautions were as described previously (Jackson-Lewis and Przedborski, 2007). To evaluate the effects of memantine (MEM) in MPTP-injected animals, mice were assigned to three different groups: CTL, MPTP, and MPTP + MEM. In the MPTP + MEM group, MEM (10 mg/kg, i.p.; QD) treatment was provided for 28 d after 5 d of MPTP injections. Further experiments were performed by blinded researchers.

NR2D KO C57BL/6N mice (Ikeda et al., 1995) were provided by RIKEN BioResource Research Center (RBRC01840) through the National Bio-Resource Project of the Ministry of Education, Culture, Sports, Science and Technology (MEXT), Japan. Genomic analyses were conducted in all animals at approximately three weeks of age. Mice were classified by genotype (Hetero, WT, and KO) and allocated to WT and KO groups. Tail genomic DNA was amplified using primer 1 (5′-GC AGGCCCCTGCCTCCTCGCTC-3′), primer 2 (5′-TGGATTGCACG CAGGTTCTC-3′), and primer 3 (5′-CTGACCTCATCCTCAGATG AG-3′). The nested polymerase chain reaction products from WT (primer 1 + primer 3) and NR2D KO (primer 1 + primer 2) mice were 281 and 982 bp long, respectively. All animals had *ad libitum* access to food throughout the experiments.

Electrophysiology and data analysis

Horizontal midbrain slices (300 µm) containing SNpc were prepared as previously described (Krashia et al., 2017). Mice were anesthetized with avertin (250 mg/kg, i.p.) and decapitated, and the brains were rapidly removed. The midbrain sections were prepared in ice-cold oxygenated (95% O_2/5% CO_2) artificial CSF (aCSF; 126 mM NaCl, 26 mM $NaHCO_3$, 5 mM KCl, 1.2 mM NaH_2PO_4, 10 mM D-glucose, 2.4 mM $CaCl_2$, 1.2 mM $MgCl_2$, pH 7.3–7.4, 305–315 mOsm) using a Vibratome (VT 1200S; Leica). Sectioned slices were kept in a slice holder containing oxygenated aCSF in the presence of 3 μM glutamic acid and incubated for 1 h at 34°C. After incubation, slices were transferred to a recording chamber that was continuously perfused with aCSF saturated with 95% O_2 and 5% CO_2 at a flow rate of 4 ml/min at 32–34°C.

For electrophysiological recording, patch pipettes (4–5 MΩ) were prepared from borosilicate glasses using a Flaming/Brown micropipette puller (Sutter Instruments) and filled with solution containing 130 mM K-gluconate, 10 mM KCl, 10 mM HEPES, 10 mM EGTA, 5 mM Mg^{2+}ATP, and 0.9 mM $MgCl_2$ (pH 7.3–7.4). The Axopatch 200B amplifier (Molecular Devices) was used for electrophysiological recording. Currents were filtered at 1 kHz and digitized at 10 kHz using the Digidata 1440A digitizer and pClamp 10.2 software (Molecular Devices). Current was recorded using the whole-cell patch-clamp technique in the presence of picrotoxin (300 μM). Series resistance was monitored continuously throughout the recording. If series resistance changed by >20%, the experiments were stopped.

The NMDA receptor-mediated tonic current (tonic I_{NMDA}) was defined as a change in the holding current ($I_{holding}$) measured as the average of 0.5-min steady-state baseline segments after the application of NMDAR antagonists. To assess tonic I_{NMDA}, we performed hierarchical testing. In the first step, we used the Shapiro–Wilk test to test the null hypothesis of a normal data distribution at a significance level of 5%. For normally distributed data, we performed one-way repeated measures-ANOVA (RM-ANOVA) followed by a *post hoc* Bonferroni's test. Tonic I_{NMDA} was recorded at a holding voltage ($V_{holding}$) of −70 or −45 mV and categorized as Mg^{2+}-resistant tonic I_{NMDA} (recorded in normal aCSF containing 1.2 mM $MgCl_2$) or Mg^{2+}-sensitive tonic I_{NMDA} (recorded in aCSF with 20 μM Mg^{2+}; Neupane et al., 2021).

Drugs were added to the perfusing aCSF solution at known concentrations. The final concentration of dimethylsulfoxide (DMSO) used to dissolve drugs was <0.05%. D-(-)−2-amino-5-phospho-nopentanoic acid (D-AP5), PPDA, TBOA, and ifenprodil were purchased from Tocris Bioscience. All other drugs were purchased from Sigma-Aldrich.

Identification of DA neurons

DA neurons were identified based on their location, morphologic appearance, and the presence of hyperpolarization-activated inward currents (I_h), shown by sag formation in response to hyperpolarizing current of −500 to −700 pA in current-clamp mode after voltage clamp recording (Fig. 1). Neurons showing sag formation and hyperpolarization of amplitude ≥50 mV with −700-pA current injection were considered as DA neurons. Approximately 60% of recorded cells in the SNpc were identified as DA neurons.

Western blotting

The midbrain substantia nigra was isolated under a stereomicroscope (Castelli et al., 2020). Proteins from the dissected midbrain substantia nigra were lysed with 1× passive lysis buffer (Cell Signaling Technology) and quantified using a Coomassie Protein assay kit (Bio-Rad). Approximately 50 μg of protein was electrophoresed on 10% sodium dodecyl sulfate–polyacrylamide gel and transferred onto nitrocellulose membranes. The blots

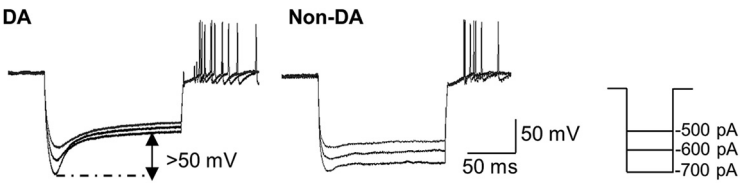

Figure 1. Characteristic hyperpolarization and sac formation because of hyperpolarization-activated inward (I_h) current in DA neurons in current-clamp mode. DA, dopaminergic neurons; non-DA, nondopaminergic neurons.

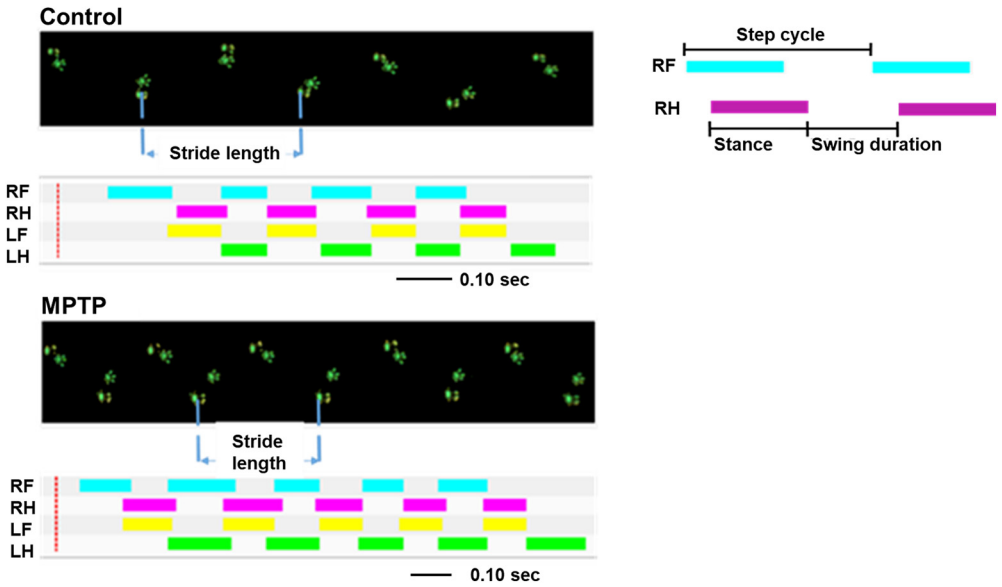

Figure 2. Representative paw prints of control mice (upper) and 1-methyl-4-phenyl-1,2,3,6-tetrahydropyridine (MPTP)-injected mice (lower) on a glass walkway during automated gait analysis. Figure graphically depicts step cycle, stance, and swing duration. RF, right front; RH, right hind; LF, left front; LH, left hind leg.

were blocked with TBST (0.1 % Tween 20 in 1X Tris-buffered saline) containing 5% skimmed milk for 1 h at room temperature (Invitrogen, Billings, MT, USA). The blots were then incubated at 4°C with primary antibodies against NMDAR NR2B (1:1000; catalog #06-600; RRID: AB_310193; Millipore), and NR2D subunits (1:1000; catalog #AGC-020; RRID: AB_10658334; Alomone Labs) diluted in TBST containing 5% skim milk. The blots were then incubated with horseradish peroxidase-conjugated goat anti-rabbit (catalog #7074; RRID: AB_2099233; Cell Signaling Technology) and anti-mouse (catalog #31430; RRID: AB_228307; Thermo Fisher Scientific) secondary antibodies (1:1000). A Pierce enhanced chemiluminescence detection kit (Thermo Fisher Scientific) was used to visualize antibody binding, and the intensity of the bands was measured using ImageJ v1.42q (National Institutes of Health).

Immunohistochemical staining

Animals were transcardially perfused with PBS containing 0.5% sodium heparin (10 U/ml) and fixed with 4% paraformaldehyde. Fixed brains were dissected from the skull, kept in 4% paraformaldehyde (10 ml) at 4°C for 10 h for postfixation, and then stored at 4°C in 30% sucrose solution (40 ml) in PBS until they sank. Next, the brains were embedded in optimal cutting temperature compound and stored at −70°C. Coronal sections (30 µm) encompassing the entire midbrain were prepared as described previously (Chung et al., 2011). Six separate series were collected, with each containing five sections (the first five sections were in the first series and so on). Subsequent immunostaining of one section from each series was performed using the free-floating method. Brain sections were treated with 3% hydrogen peroxidase (3% H_2O_2), rinsed in PBS, and nonspecific bindings were blocked with 1% BSA. The sections were permeabilized with 1% PBS containing 0.01% Triton X-100 (PBST) and incubated overnight at 4°C with a primary antibody directed against tyrosine hydroxylase (TH; 1:1000; catalog #P40101-150; Pel Freeze Biologicals; RRID: AB_2617184). The following day, they were rinsed with PBST and incubated with a secondary antibody, anti-rabbit IgG HRP-linked antibody (1:1000; catalog #7074; Cell Signaling Technology; RRID: AB_2099233) for 1 h at room temperature. Immunoreactivity was visualized by treating the tissue with 0.03% of a 3-3'-diaminobenzidine tetrahydrochloride (DAB-HCl) enhanced liquid substrate system for 10 min. Stained tissue sections were mounted on gelatin-coated slides. TH-positive neurons in the SNpc region were counted manually using a standard stereological method (S.R.W. Stott and Barker, 2014). The definition of substantia nigra used in this study was described previously (S.R.W. Stott and Barker, 2014; S.R. Stott et al., 2017). Neurons throughout the SNpc were counted, with one section chosen at random from each series of slices. Cells were counted in both hemispheres under a 40× objective bright field microscope (Olympus) fitted with a CCD-100 camera (DAGE-MTI), and the average count for both sides of each slice was multiplied by 6. This procedure was applied to four slices randomly selected from remaining four different series and the total number of TH-positive neurons was calculated.

Automated gait analysis

We analyzed the gait parameters of voluntarily moving mice using the CatWalk XT system (Noldus Information Technology), as previously described (Deumens et al., 2006; Koopmans et al., 2007). Before baseline testing, the mice were well trained to walk on a glass walkway (30 cm long, 5.5 cm wide) that illuminated the area of paw contact with green light (Fig. 2). After baseline testing, drug injections were started according to the drug injection schedule, previously explained in the Animal experiments section. Gait parameters were tested on days 14, 21, and 28 after the last dose of MPTP. A high-speed video camera captured the footprints of the mice during walking and the CatWalk XT system

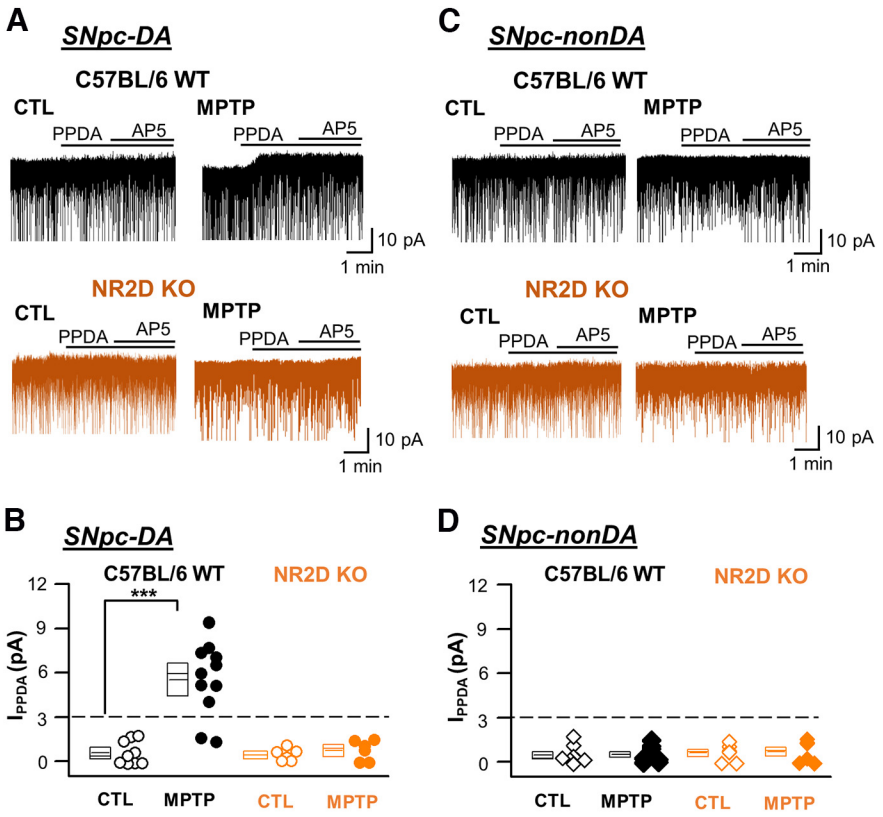

Figure 3. NR2D knock-out (KO) selectively prevents MPTP-induced Mg^{2+}-resistant tonic I_{NMDA} in substantia nigra pars compacta (SNpc) DA versus non-DA neurons. ***A***, Representative traces of SNpc DA neurons from the control (CTL) and MPTP-injected groups showing the outward shift in the holding current ($I_{holding}$) induced by PPDA (1 μM) followed by the addition of AP5 (100 μM) in wild-type (WT) and NR2D KO mice. ***B***, Summarized amplitudes of PPDA-sensitive I_{NMDA} in DA neurons in control and MPTP-injected WT (***$p < 0.001$, WT-CTL vs WT-MPTP, two-sample Student's t test, $n = 9$ and 11, respectively, from 6 or 7 mice) and NR2D KO mice ($p = 0.270$, KO-CTL vs KO-MPTP, two-sample Student's t test, $n = 6$ in each group, from 5 mice). Experiments were performed 3 d after the MPTP injection. ***C***, Representative traces showing PPDA-sensitive tonic I_{NMDA} in SNpc non-DA neurons from WT and NR2D KO mice. ***D***, Summarized amplitudes of PPDA-sensitive tonic I_{NMDA} in SNpc non-DA neurons in control and MPTP-injected mice ($n = 6$ in each group from 4 to 6 mice).

automatically calculated multiple gait parameters, such as stride length, stance, run duration, and cadence.

The gait parameters described below were taken from the reference manual provided by the manufacturer, and were congruous with previous studies (X.H. Wang et al., 2012; M. Zhou et al., 2015). The stride length (cm) was the distance between two successive points of contact of the same paw. The stance (s) was the duration of contact of a paw with the glass plate. The run duration (s) was the duration of an entire run. The cadence (steps/s) was the number of steps in 1 s.

Y maze spontaneous alternation task

Spontaneous alternation performance was tested as described previously (Park et al., 2022) to assess the hippocampus-dependent spatial working memory. Each mouse was placed in the center of a symmetrical Y maze and allowed to explore the maze freely during an 8 min session. The total number and sequence of arm entries were recorded and analyzed. Arm entry was defined as the hind paws of the mice being completely within the arm. The percentage of alternation refers to the number of trials involving entries into all three arms divided by the maximum possible number of alternations (total number of arms entered − 2) × 100.

Statistical analysis and experimental design

Plots were generated using Microcal Origin software (OriginLab; RRID: SCR_002815). Numerical data are presented as mean ± SEM. Normality of data were determine using Shapiro–Wilk test. Normally distributed data were assessed with parametric tests: two-sample Student's t test, paired-sample Student's t test or ANOVA followed by a *post hoc* test (e.g., Bonferroni's test). In case data were not normally distributed, we used nonparametric tests: Mann–Whitney test and Wilcoxon signed-rank tests. Group data were expressed as box plots, indicating the median (thick centerline), mean (thin line), and SEM (box edges). Male mice were used for all experiments to avoid effects of hormones on the results. Electrophysiological recordings were conducted in three or more animals per group, and two to three slices were collected per animal. To compare protein (NR2B and NR2D) expression levels in the CTL and the MPTP groups, we used a one-way ANOVA followed by a *post hoc* test. The effects of MEM and genetic KO of NR2D in cell death and gait behaviors were compared using a two-way RM-ANOVA followed by a *post hoc* test.

Results

Chronic pathologic stimuli recruited NR2D-containing eNMDARs that generated an Mg^{2+}-resistant tonic I_{NMDA} in the mature brain, which has been found to regulate neuronal activity in a cell type-specific manner (Neupane et al., 2021). To investigate whether this phenomenon plays a role in midbrain DA neuronal loss, we measured Mg^{2+}-resistant tonic I_{NMDA}, and compared the results for DA and non-DA neurons from control and MPTP-injected mice (3 d after 5 d of MPTP injection).

MPTP selectively generates an Mg^{2+}-resistant tonic I_{NMDA} in SNpc DA but not non-DA neurons

We compared Mg^{2+}-resistant tonic I_{NMDA} in SNpc DA neurons identified by the sequential application of an NR2C/D-selective NMDAR antagonist, (2R*,3S*)−1-(phenanthrenyl-2-carbonyl) piperazine-2,3-dicarboxylic acid (PPDA; Feng et al., 2004), and additional AP5 (Fig. 3*A*,*B*). PPDA (1 μM) and additional AP5 (PPDA + AP5) failed to cause significant $I_{holding}$ changes in the control group ($F_{(2,24)} = 2.97$, $p = 0.10$, $n = 9$ neurons from five

Table 1. Phasic current properties of SNpc DA neurons

	n	EPSC Freq. (Hz)	EPSC Amp. (pA)	Weighted τ (ms)
WT-CTL				
aCSF	7	1.29 ± 0.26	30.04 ± 1.38	5.02 ± 0.61
PPDA	7	1.09 ± 0.44	29.37 ± 1.47	4.83 ± 0.76
WT-MPTP				
aCSF	7	1.30 ± 0.19	32.43 ± 2.86	5.43 ± 1.07
PPDA	7	1.22 ± 0.18	30.36 ± 2.79	5.46 ± 0.79
KO-CTL				
aCSF	6	1.17 ± 0.14	28.34 ± 2.74	5.55 ± 0.45
PPDA	6	1.33 ± 0.15	27.75 ± 2.72	5.49 ± 0.58
KO-MPTP				
aCSF	6	1.13 ± 0.28	30.86 ± 3.05	5.47 ± 1.28
PPDA	6	1.16 ± 0.25	28.55 ± 1.72	5.35 ± 1.11

n: numbers of recorded cells.
WT: C57BL/6-WT; KO: C57BL/6-NR2D-KO; CTL: saline injection; MPTP: MPTP injection.
Freq., frequency; Amp., amplitude.

mice, one-way RM-ANOVA). By contrast, PPDA caused a significant outward shift in $I_{holding}$ (I_{PPDA}) in 9 of 11 tested neurons from the 3 d post-MPTP group (6.44 ± 0.53 pA, $F_{(2,24)} = 95.25$, $n = 9$ from seven mice; 5.53 ± 0.75, $F_{(2,30)} = 51.37$, $n = 11$ of all tested neurons, $p < 0.001$, Bonferroni's *post hoc* test following one-way RM-ANOVA in both case), whereas the subsequent addition of AP5 (PPDA + AP5) failed to induce a further $I_{holding}$ shift in all tested neurons ($p = 0.55$, Bonferroni's *post hoc* test). Unfortunately, we were unable to obtain stable recordings in SNpc DA neurons 5 d after the MPTP injection.

Interestingly, PPDA and additional AP5 (PPDA + AP5) caused only minimal $I_{holding}$ changes in all tested SNpc non-DA neurons, in both the control ($F_{(2,21)} = 2.54$, $p = 0.13$, $n = 8$ neurons from seven mice, one-way RM-ANOVA) and MPTP groups ($F_{(2,21)} = 2.74$, $p = 0.13$, $n = 8$ neurons from seven mice, one-way RM-ANOVA; Fig. 3*C*,*D*). This finding supports the idea that state-dependent recruitment of NR2D-containing eNMDARs generates Mg^{2+}-resistant tonic I_{NMDA} in a cell type-specific manner (Neupane et al., 2021).

In the next experiment, we investigated whether MPTP generated Mg^{2+}-resistant tonic I_{NMDA} in SNpc DA neurons in WT versus NR2D KO mice. As summarized in Figure 3*A–D*, PPDA and additional AP5 failed to uncover Mg^{2+}-resistant tonic I_{NMDA} in all tested DA (Control: $F_{(2,15)} = 3.71$, $p = 0.09$; MPTP: $F_{(2,15)} = 3.57$, $p = 0.11$, one-way RM-ANOVA) and non-DA neurons (Control: $F_{(2,15)} = 3.96$, $p = 0.08$; MPTP: $F_{(2,15)} = 3.89$, $p = 0.11$, one-way RM-ANOVA, $n = 6$ neurons in each group from four mice) from NR2D KO mice. This finding implies that NR2D-containing NMDARs play an essential role in the generation of Mg^{2+}-resistant tonic I_{NMDA} in MPTP-treated SNpc DA neurons.

Given that glutamate overspill may affect the ambient glutamate concentration, it may also affect I_{NMDA} (Wild et al., 2015). To determine whether this is the case in SNpc DA neurons in the mature brain, we compared the effects of PPDA on spontaneous EPSCs (sEPSCs) between WT and NR2D KO mice (Table 1). The main characteristics of sEPSCs, including the frequency, were not different between WT and NR2D KO mice, and there were no effects of MPTP injection in either group. Furthermore, PPDA did not affect sEPSCs in any group (Table 1), suggesting that changes in presynaptic glutamate release are not the cause of the Mg^{2+}-resistant tonic I_{NMDA} of SNpc DA neurons in MPTP groups.

MPTP-induced Mg^{2+}-resistant tonic I_{NMDA} in VTA DA neurons

In PD, motor manifestations are primarily linked to the selective loss of SNpc DA neurons (Brichta et al., 2013). In contrast, very similar DA neurons in the ventral tegmental area (VTA) demonstrate a higher degree of resistance to degeneration (Dauer and Przedborski, 2003). To investigate a possible role of NR2D in the differential vulnerability of SNpc and VTA neurons in MPTP induced neuronal toxicity, we measured Mg^{2+}-resistant tonic I_{NMDA} in VTA DA and non-DA neurons and compare them with from control and MPTP group (Fig. 4).

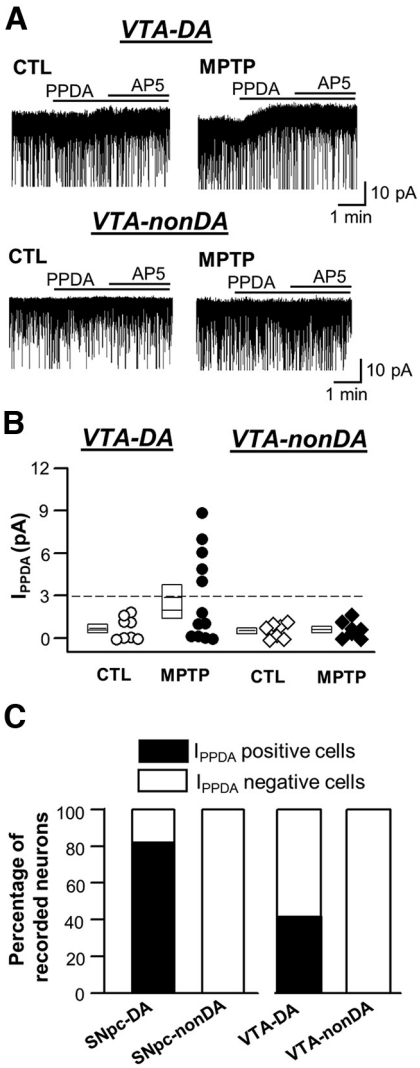

Figure 4. MPTP-induced Mg^{2+}-resistant tonic I_{NMDA} in ventral tegmental area (VTA) DA and non-DA neurons. ***A***, Representative traces of DA and non-DA neurons in the VTA from the control (CTL) and MPTP groups showing the outward shift in $I_{holding}$ induced by PPDA (1 μM), followed by the addition of AP5 (100 μM), in WT mice. ***B***, Amplitudes of PPDA-sensitive I_{NMDA} in VTA DA and VTA non-DA neurons in control and MPTP-injected WT mice ($p = 0.13$, WT-CTL vs WT-MPTP, Mann–Whitney test, $n = 8$ and 12, respectively, from 7 mice in each group). The experiments were performed 3 d after MPTP injection. ***C***, Bar graph showing the proportions of PPDA-positive and PPDA-negative neurons (percentage of total recorded neurons in each group) in the SNpc and VTA in MPTP-injected WT mice.

PPDA (1 μM) and additional AP5 (PPDA + AP5) caused minimal $I_{holding}$ changes in both VTA DA ($F_{(2,21)} = 3.22$, $p = 0.11$, one-way RM-ANOVA) and non-DA neurons of control ($F_{(2,21)} = 2.88$, $p = 0.13$, one-way RM-ANOVA, $n = 8$ neurons from five mice in each group; Fig. 4*A*). As expected, PPDA and additional AP5 (PPDA + AP5) failed to induce a significant shift in $I_{holding}$ of VTA non-DA neurons in the MPTP group ($F_{(2,18)} = 3.14$, $p = 0.10$, one-way RM-ANOVA, $n = 7$ neurons from five mice). By contrast, PPDA revealed Mg^{2+}-resistant tonic I_{NMDA} in five of 12 tested VTA DA

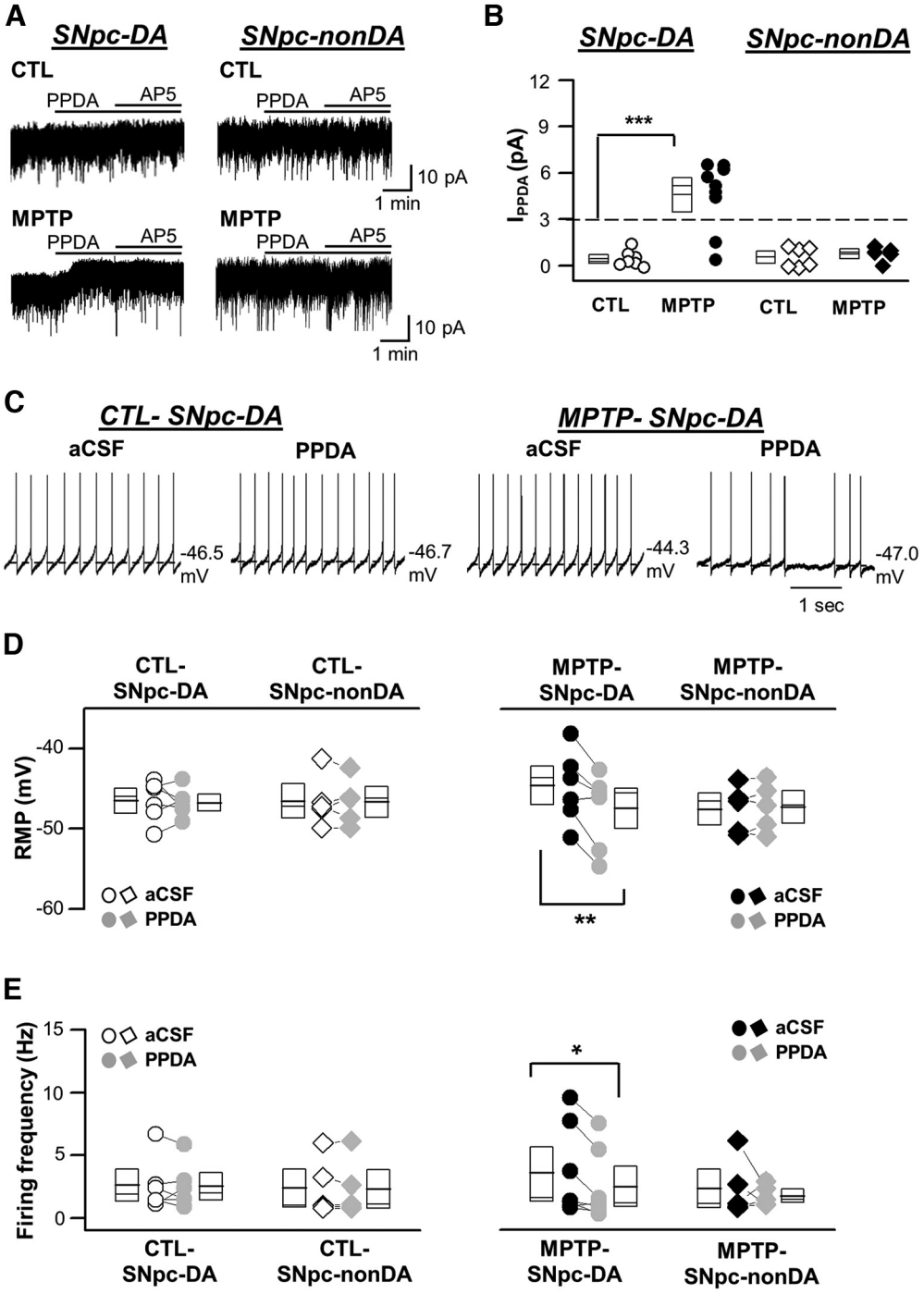

Figure 5. MPTP-induced Mg^{2+}-resistant tonic $I_{NMDA\ at}$ resting membrane potential (V_m) of SNpc DA and non-DA neurons. ***A***, Representative traces of DA and non-DA neurons of SNpc from the CTL and MPTP groups showing the outward shift in $I_{holding}$ induced by PPDA (1 μM) followed by the addition of AP5 (100 μM) in WT mice at resting potential (−45 mV). ***B***, Summarized amplitudes of PPDA-sensitive I_{NMDA} in DA and non-DA neurons in control and MPTP-injected WT mice at resting V_m (−45 mV; ***$p < 0.001$, WT-CTL vs WT-MPTP, two-sample Student's *t* test, $n = 7$ and 9, respectively, from 6 or 7 mice). ***C***, Representative traces of neuronal firing in DA neurons of SNpc from the CTL and MPTP groups. ***D***, Summarized bar graph showing resting V_m changes induced by PPDA in DA and non-DA neurons in SNpc from the CTL and MPTP groups (**$p < 0.01$, aCSF, paired-sample Student's *t* test, $n = 5$–7 from 5 mice in each group). ***E***, Summarized bar graph showing neuronal firing changes induced by PPDA in DA and non-DA neurons in SNpc from the CTL and MPTP groups (*$p < 0.05$, aCSF, Wilcoxon signed-rank test, $n = 6$–7 from five mice in each group).

neurons in MPTP group (6.13 ± 0.84 pA, $F_{(2,12)} = 33.74$, $n = 5$ from five mice, 2.87 ± 0.90, $F_{(2,33)} = 11.59$, $n = 12$ from eight mice, $p < 0.01$, Bonferroni's *post hoc* test following one-way RM-ANOVA in both case), and additional AP5 (PPDA + AP5) failed to induce a further $I_{holding}$ shift in all tested cells ($p = 0.84$, Bonferroni's *post hoc* test).

Notably, the PPDA-induced $I_{holding}$ shift was within the range of control values in some VTA and SNpc DA neurons of the MPTP group (Fig. 4*C*). However, the proportion of DA neurons showing I_{PPDA} within the range of control values (1.7 pA maximally) was significantly lower in SNpc (18.2%, 2 of 11) than VTA region [59% (7 of 12), $p = 0.04$, two-tailed χ^2 test].

MPTP induces an Mg^{2+}-resistant tonic I_{NMDA} near the resting membrane potential (V_m) of SNpc DA neurons

In next experiments, we investigated whether MPTP generates tonic I_{NMDA} at the resting membrane potential (RMP; −45 mV) of SNpc DA neurons (Otomo et al., 2020) . Even at a $V_{holding}$ of −45 mV, PPDA caused an outward shift in the $I_{holding}$ of SNpc DA neurons in the MPTP group (4.58 ± 0.73 pA, $n = 12$ neurons from six mice, $F_{(2,24)} = 37.06$, $p < 0.001$, Bonferroni's *post hoc* test following one-way RM-ANOVA; Fig. 5*A*,*B*). The subsequent addition of AP5 (PPDA + AP5) failed to induce a further shift in $I_{holding}$ ($p = 0.76$, Bonferroni's *post hoc* test). By contrast, both PPDA and additional AP5 (PPDA + AP5) caused no significant $I_{holding}$ changes in control SNpc DA neurons ($F_{(2,18)} = 3.46$, $p = 0.08$, one-way RM-ANOVA, $n = 9$ from eight mice). Similar to $V_{holding}$ of −70 mV (Fig. 3), PPDA and additional AP5 caused only minimal $I_{holding}$ changes in non-DA neurons of the control ($F_{(3,12)} = 4.05$, $p = 0.10$, $n = 5$ neurons from five mice) and MPTP groups ($F_{(2,15)} = 3.28$, $p = 0.11$, one-way RM-ANOVA, $n = 6$ neurons from four mice).

Given that MPTP induced tonic I_{NMDA} at RMP, −45 mV, it is plausible that extrasynaptic NR2D recruitment regulates the V_m of SNpc DA neurons. We compared the effects of PPDA on V_m in control and MPTP groups (Fig. 5*A*,*B*). MPTP injection did not affect RMP of SNpc DA (Control: −46.51 ± 1.03 mV, $n = 6$ neurons from six mice; MPTP: −44.50 ± 1.58 mV, $n = 7$ from six mice) and non-DA neurons (Control: −46.53 ± 1.41 mV, $n = 5$ neurons from five mice; MPTP: −47.48 ± 1.31 mV, $n = 5$ from four mice; $F_{(3,20)} = 0.14$, $p = 0.70$, two-way RM-ANOVA). However, PPDA significantly hyperpolarized the V_m in the MPTP group (aCSF: −44.50 ± 1.58 mV; PPDA: −47.37 ± 1.67 mV, $p < 0.01$, paired-sample Student's *t* test) but not in the control group (aCSF: −46.51 ± 1.03 mV; PPDA: −46.73 ± 0.85 mV, $p = 0.80$, paired-sample Student's *t* test). PPDA did not cause any significant changes in the V_m of non-DA neurons in the control or MPTP groups.

In addition, PPDA significantly decreased the neuronal firing rate in SNpc DA neurons in the MPTP groups (aCSF: 3.58 ± 1.36 Hz; PPDA: 2.46 ± 1.06 Hz, $n = 7$ neurons from five mice, $p = 0.03$, Wilcoxon signed-rank test), while it caused a minimal changes in SNpc DA neurons in the control group (aCSF: 2.95 ± 1.17 Hz; PPDA: 2.52 ± 0.72 Hz, $n = 6$ neurons from five mice, $p = 0.60$, Wilcoxon signed-rank test; Fig. 3*C*,*E*). PPDA did not cause any significant changes in the neuronal firing of SNpc non-DA neurons in the control or MPTP groups (Fig. 3*C*,*E*). Meanwhile, MPTP injection or PPDA did not affect input resistance of both SNpc DA and non-DA neurons (Table 2). These results indicate that NR2D-containing eNMDARs generate Mg^{2+}-resistant tonic I_{NMDA} to set the resting V_m, thereby regulating the neuronal excitability and or excitotoxicity of SNpc DA neurons in MPTP-injected mice.

NR2B does not contribute to MPTP-induced Mg^{2+}-resistant tonic I_{NMDA} in SNpc neurons

We used ifenprodil, a selective antagonist of the NR2B subunit (Chenard and Menniti, 1999), to investigate the role(s) of NR2B in MPTP-induced Mg^{2+}-resistant tonic I_{NMDA} in SNpc neurons. Ifenprodil caused minimal $I_{holding}$ changes in both the control ($F_{(2,15)} = 3.77$, $p = 0.08$, one-way RM-ANOVA, $n = 6$ from five mice) and MPTP groups ($F_{(2,15)} = 43.32$, $n = 6$ neurons from four mice, $p = 0.70$, Bonferroni's *post hoc* test following one-way RM-ANOVA), while additional AP5 (ifenprodil + AP5) uncovered Mg^{2+}-resistant tonic I_{NMDA} in the MPTP group (5.92 ± 0.97 pA, $p < 0.001$, Bonferroni's *post hoc* test following one-way RM-ANOVA) but not in the control group (Fig. 6*A*,*B*). By contrast, MEM, which is an NMDAR antagonist that preferentially targets extrasynaptic receptors (Xia et al., 2010; Wu and Johnson, 2015), uncovered Mg^{2+}-resistant tonic I_{NMDA} in MPTP (5.31 ± 1.0 pA, $F_{(2,15)} = 17.68$, $n = 7$ neurons from five mice, $p < 0.001$, Bonferroni's *post hoc* test following one-way RM-ANOVA) but not in control mice ($F_{(2,15)} = 3.91$, $p = 0.10$, one-way RM-ANOVA, $n = 6$ neurons from five mice). The subsequent addition of AP5 (MEM + AP5) did not induce a further shift in $I_{holding}$ in either group (Fig. 6*A*,*B*).

In the next experiment, we compared the protein expression of the NR2B and NR2D subunits in SNpc before and after MPTP injection. Western blotting analysis showed the presence of both NR2B and NR2D in the nucleus (Fig. 6*C*,*D*). Importantly, NR2D-subunit polypeptide expression was significantly higher in both the 3 d (2.71 ± 0.20 times that of the control) and 7 d post-MPTP groups (3.54 ± 0.56 times that the of control, $F_{(2,18)} = 13.66$, $p < 0.001$, in both case, Bonferroni's *post hoc* test following one-way ANOVA), whereas NR2B expression was similar among all three groups ($F_{(2,15)} = 3.14$, $p = 0.07$, one-way ANOVA). These results support the idea that MPTP selectively recruited NR2D- over NR2B-containing eNMDARs to generate an Mg^{2+}-resistant tonic I_{NMDA} in SNpc DA neurons.

Table 2. Input resistance (IR) and series resistance (SR) of SNpc DA and non-DA neurons

		IR (mΩ)		
	n	aCSF	PPDA	SR (mΩ)
DA				
Control	9	556.97 ± 39.89	573.50 ± 40.29	12.01 ± 0.30
MPTP	11	526.49 ± 21.15	548.21 ± 24.63	13.44 ± 0.56
Non-DA				
Control	8	543.72 ± 29.62	550.78 ± 40.70	11.87 ± 0.45
MPTP	8	523.77 ± 37.43	547.13 ± 39.82	12.56 ± 0.81

Increased ambient glutamate is not sufficient to generate MPTP-induced Mg^{2+}-resistant tonic I_{NMDA} in SNpc DA neurons

To verify whether extrasynaptic NR2D recruitment is essential for the generation of MPTP-induced Mg^{2+}-resistant I_{NDMA} in SNpc DA neurons, we measured Mg^{2+}-resistant I_{NMDA} under increased ambient glutamate conditions induced by EAAT blockade or exogenous glutamate (Fig. 7).

A broad-spectrum EAAT antagonist, TBOA (100 μM), induced a similar inward shift in the $I_{holding}$ of SNpc DA neurons in control (13.8 ± 3.14 pA, $n = 5$ neurons from five mice, and MPTP groups (14.32 ± 2.67 pA, $n = 5$ neurons from four mice, $p = 0.90$ compared with control, two-sample Student's *t* test). Even in the presence of TBOA, AP5 caused minimal changes in the $I_{holding}$ of control SNpc DA neurons ($F_{(2,12)} = 18.63$, $p = 0.69$, Bonferroni's *post hoc* test). By contrast, AP5 uncovered the Mg^{2+}-resistant tonic I_{NMDA} in MPTP groups (7.34 ± 1.52 pA, $F_{(2,12)} = 18.04$, $n = 5$ neurons from four mice, $p < 0.001$, Bonferroni's *post hoc* test; Fig. 7*A*,*B*), which was comparable to the I_{PPDA} in normal aCSF (6.44 ± 0.53 pA, $n = 9$, $p = 0.51$ compared with control, two-sample Student's *t* test).

In an agreement, PPDA and additional AP5 (PPDA + AP5) caused minimal changes in the $I_{holding}$ of control SNpc DA neurons in the presence of both 100 μM TBOA ($F_{(2,12)} = 2.80$, $p = 0.16$, one-way RM-ANOVA, $n = 5$ neurons from four mice) and 30 μM glutamate ($F_{(2,15)} = 3.07$, $p = 0.12$, one-way RM-ANOVA, $n = 6$ neurons from four mice; Fig. 7*C*). These results

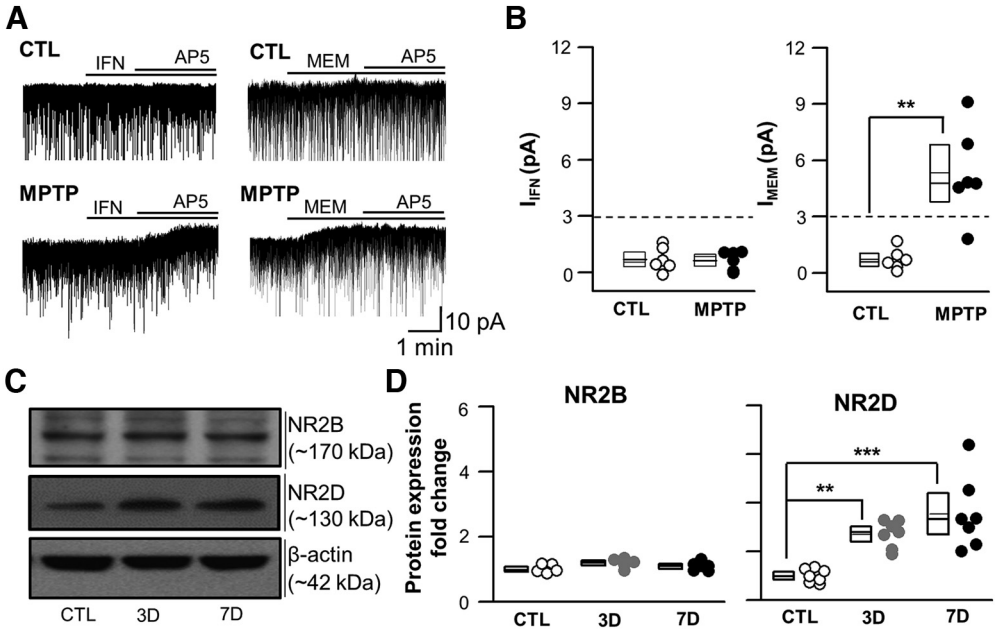

Figure 6. Pharmacological properties of MPTP-induced tonic I_{NMDA} in nondepolarized SNpc DA neurons. ***A***, Representative traces of DA neurons from CTL and MPTP mice, showing the outward shift in $I_{holding}$ induced by ifenprodil (IFD: 30 μM) and memantine (MEM; 30 μM) followed by the addition of AP5 (100 μM). ***B***, Summarized IFD-sensitive and MEM-sensitive tonic I_{NMDA} for the control (CTL) and MPTP groups (I_{IFD}; $p = 0.87$, CTL vs MPTP, two-sample Student's *t* test, $n = 6$ from five mice and I_{MEM}; $^{**}p < 0.01$, CTL vs MPTP, two-sample Student's *t* test, $n = 6$ from 5 mice). ***C***, Representative Western blot analysis results showing NMDAR NR2B and NR2D subunit expression in the SNpc of the CTL and MPTP groups. ***D***, NR2B and NR2D subunit expression in the SNpc in the CTL and MPTP groups, respectively. Protein expression was normalized to the level detected in the CTL group and compared with the expression in MPTP animals (NR2B: one-way ANOVA, $F_{(2,15)} = 3.14$, $p > 0.05$, $n = 6$ and NR2D: one-way ANOVA, $F_{(2,\ 18)} = 13.66$, $p < 0.001$, $^{**}p < 0.01$, $^{***}p < 0.001$, compared with control, Bonferroni's *post hoc* test, $n = 7$ mice).

supported the idea that increased ambient glutamate is not enough to generate the Mg^{2+}-resistant tonic I_{NMDA} in SNpc DA neurons.

In the next experiment, we adopted low $[Mg^{2+}]_o$ aCSF to investigate whether Mg^{2+} unblock could uncover PPDA-sensitive I_{NDMA} in SNpc DA neurons. Even in low $[Mg^{2+}]_o$ aCSF, PPDA failed to affect $I_{holding}$ in control mice ($F_{(2,15)} = 38.54$, $p = 1.0$, Bonferroni's *post hoc* test following one-way RM-ANOVA), while additional AP5 (PPDA + AP5) uncovered an Mg^{2+}-sensitive tonic I_{NMDA} (9.19 ± 1.61 pA, $n = 6$ from five mice, $p < 0.001$, *post hoc* Bonferroni's test). By contrast, PPDA caused a significant $I_{holding}$ shift in MPTP-treated mice (5.77 ± 0.48, $F_{(2,15)} = 121$, $n = 6$ neurons from four mice, $p < 0.001$, Bonferroni's *post hoc* test following one-way RM-ANOVA), and additional AP5 (PPDA + AP5) further uncovered an Mg^{2+}-sensitive tonic I_{NMDA} (8.91 ± 1.16, $p < 0.001$, *post hoc* Bonferroni's test), which was comparable to that of control SNpc DA neurons ($p = 0.88$, two-sample Student's *t* test). These results suggested that MPTP necessarily recruited additional extrasynaptic NR2D-containing NMDARs to generate the Mg^{2+}-resistant tonic I_{NMDA} in SNpc DA neurons.

Inhibition of NR2D attenuates MPTP-induced SNpc DA neuronal loss

To verify the role of NR2D-containing eNMDARs in MPTP-induced Parkinsonism, we used immunoreactivity against anti-tyrosine hydroxylase (TH) antibody, which is the gold standard for identifying DA neurons in the midbrain (Sawamoto et al., 2001; White and Thomas, 2012), we compared the MPTP-induced DA neuronal loss in SNpc from WT and NR2D KO mice (Fig. 8).

As expected, MPTP-induced DA neuronal loss was significantly attenuated in NR2D KO mice ($F_{(1,40)} = 27.08$, $p = 0.01$, two-way RM-ANOVA). The numbers of SNpc DA neurons were not different in control WT and NR2D KO mice (WT: 6238.28 ± 177.52 and KO: 6287.12 ± 312.79, $n = 6$ in each group, $p = 0.88$, Bonferroni's *post hoc* test), which indicated that the NR2D KO did not affect cell viability under normal conditions. MPTP significantly and gradually reduced the number of SNpc DA neurons in 3, 7, and 28 d post-MPTP in both WT and KO mice ($F_{(3,40)} = 106.93$, $p < 0.001$, two-way RM-ANOVA). However, numbers of SNpc DA neurons were not different in WT and NR2D KO mice in 3 d post-MPTP (WT: 4541.66 ± 245.53 and KO: 4980 ± 322.86, $n = 6$ in each group, $p = 0.20$, Bonferroni's *post hoc* test). Meanwhile, MPTP-induced DA neuronal loss was significantly attenuated in NR2D KO mice in 7 d post-MPTP (WT: 3652 ± 187.21 and KO: 4569.66 ± 322.56, $n = 6$ in each group, $p = 0.01$, Bonferroni's *post hoc* test) and in 28 d post-MPTP (WT: 2631.83 ± 115.42 and KO: 4020 ± 242.86, $n = 6$ in each group, $p < 0.001$, Bonferroni's *post hoc* test).

Similar results were observed with MEM, which significantly reduced MPTP-induced TH-positive neuronal loss in SNpc regions ($p < 0.05$ compared with MPTP only, Bonferroni's *post hoc* test; Fig. 8*C*). These results suggest that NR2D-containing eNMDAR mediated MPTP-induced TH-positive neuronal loss.

Inhibition of NR2D improves MPTP-induced gait deficits

SNpc DA neuronal loss is a hallmark of PD with abnormal gait (Damier et al., 1999; Michel et al., 2016), whereas VTA DA neuronal loss is involved in nonmotor symptoms, such as depression and cognitive impairment (Narayanan et al., 2013; Friedman et al., 2014; H. Wang et al., 2023). Although MPTP reportedly induced cognitive dysfunction in rodents (X. Zhang et al., 2018; Han et al., 2020), this was not seen in all studies (Da Cunha et al., 2003; Ferguson et al., 2015). In the present study, MPTP did not induce significant cognitive deficits in the Y-maze test, as indicated by the

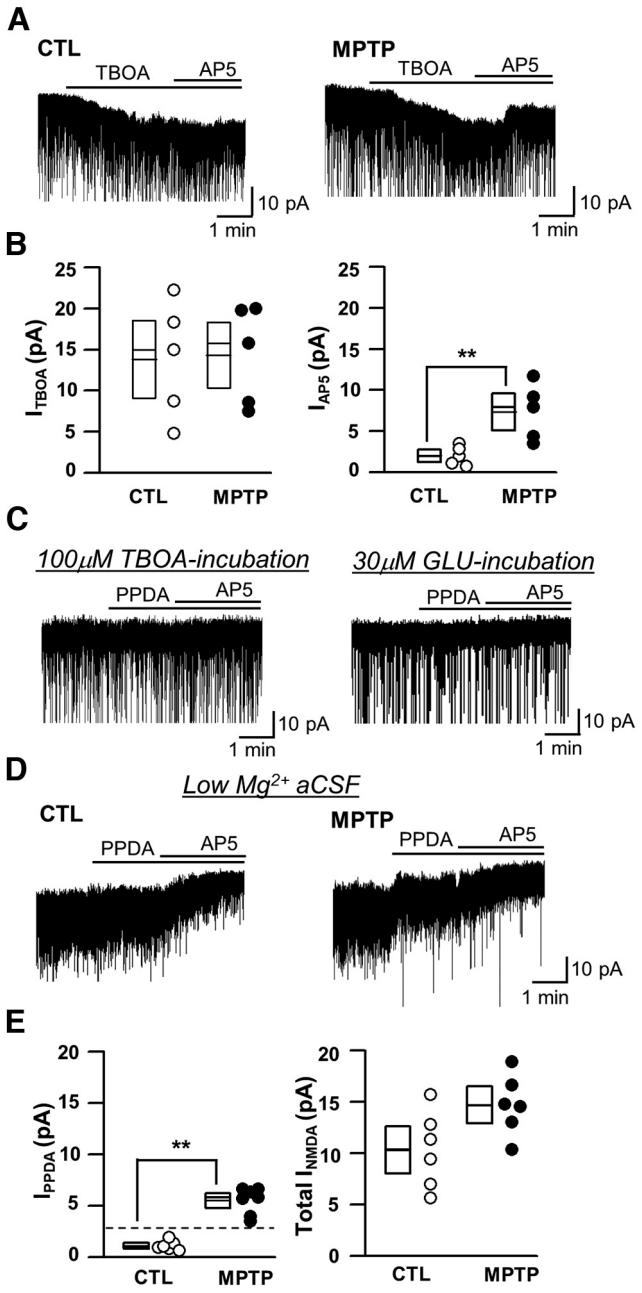

Figure 7. Increased ambient glutamate is not sufficient to generate a PPDA-sensitive tonic I_{NMDA} in SNpc DA neurons. ***A***, Representative traces of DA neurons from the control (CTL) and MPTP-injected (MPTP) groups showing the effect of glutamate transporter blocker (TBOA; 100 μM), followed by the addition of AP5 (100 μM) in holding current. ***B***, Summarized bar graph showing the mean change in the holding current after the administration of TBOA (left) and additional AP5 (right) in the control and MPTP groups (I_{TBOA}; $p = 0.90$, CTL vs MPTP, two-sample *t* test, $n = 5$ and I_{AP5}; $^{**}p < 0.01$, CTL vs MPTP, two-sample *t* test, $n = 5$ from 4 or 5 mice). ***C***, Representative traces showing a PPDA-sensitive tonic I_{NMDA} in SNpc DA neurons from WT control mice in normal aCSF containing high levels of glutamate (30 μM) and glutamate transporter blocker (TBOA; 100 μM). ***D***, Representative traces of DA neurons from the CTL and MPTP groups showing the outward shift in $I_{holding}$ induced by PPDA (1 μM) followed by the addition of AP5 (100 μM) in aCSF containing low levels of magnesium $[Mg^{2+}]_o$ (20 μM). ***E***, PPDA-sensitive tonic I_{NMDA}, summarized for the CTL and MPTP groups (I_{PPDA}; $^{**}p < 0.01$, CTL vs MPTP, Mann–Whitney test, $n = 6$ in each group and total I_{NMDA}; $^{*}p = 0.04$, CTL vs MPTP, two-sample Student's *t* test, $n = 6$ in each group from four mice).

spontaneous alteration data, in either WT or NR2D KO mice (Table 3).

To investigate the functional significance of extrasynaptic NR2D recruitment in MPTP-induced SNpc DA neuronal loss, we evaluated and compared MPTP-induced gait deficit in WT and NR2D KO mice. Using the CatWalk automated gait analysis system (Boix et al., 2018), we analyzed various gait parameters, including static (stride length), dynamic (standing duration and cadence), and general parameters (run duration). Instability because of acute MPTP toxicity precluded detailed catwalk analysis until day 14 after MPTP injection.

We observed an MPTP-induced gait deficiency in both WT and NR2D KO mice, as indicated by a prolonged run duration [WT: from 1.23 ± 0.03 s to 1.97 ± 0.07 s (14 d), 2.12 ± 0.07 s (21 d), and 2.23 ± 0.07 s (28 d); NR2D KO: from 1.16 ± 0.04 s to 1.68 ± 0.09 s (14 d), 1.58 ± 0.08 s (21 d), and 1.58 ± 0.06 s (28 d), $n = 8$–25 animals in each group, $p < 0.01$ compared with control, Bonferroni's *post hoc* test] and reduced cadence [WT: from 19.63 ± 0.53 steps/s to 15.71 ± 0.34 steps/s (14 d), 15.12 ± 0.30 steps/s (21 d), and 13.41 ± 0.45 steps/s (28 d); NR2D KO: from 19.93 ± 0.66 steps/s to 16.37 ± 0.30 steps/s (14 d), 16.18 ± 0.44 steps/s (21 d), and 16.64 ± 0.51 steps/s (28 d), $n = 8$–25 animals in each group, $p < 0.01$ compared with each control, Bonferroni's *post hoc* test]. The MPTP-induced gait deficiency was more critical in WT than in NR2D KO animals (WT-MPTP vs KO – MPTP; run duration, $p = 0.001$ and cadence, $p = 0.002$, Bonferroni's *post hoc* test following two-way ANOVA in both case; Fig. 9*A*,*B*), indicating that NR2D blockade could prevent MPTP-induced gait deficiency. Consistent with this, the NR2D KO attenuated the MPTP-induced increase in stance and decrease in stride length at 28 d post-MPTP (Tables 4, 5), suggesting that NR2D blockade attenuated DA neuron degeneration to improve MPTP-induced abnormal gait.

In agreement, eNMDAR blocker MEM (Xia et al., 2010; Wu and Johnson, 2015), significantly improved gait deficiency indicated by run duration and cadence at 21, and 28 d post-MPTP in MPTP-injected WT mice ($p < 0.01$ compared with WT-MPTP group in both 21 and 28 d, Bonferroni's *post hoc* test following one-way ANOVA; Fig. 9*A*,*B*) as well as stride length and stand duration (Tables 4, 5). MEM did not cause any changes in run duration or cadence (Fig. 9*A*,*B*), nor in stride length or stand duration (Tables 4, 5) in MPTP-injected NR2D KO mice, suggesting that MEM improved MPTP-induced abnormal gait via NR2D-containing NMDARs.

Discussion

The main findings of this study demonstrate the critical role of NR2D-containing NMDA receptors in toxin-induced parkinsonian models: MPTP intoxication selectively generated an Mg^{2+}-resistant tonic I_{NMDA} in SNpc DA neurons compared with non-DA neurons, failed to generate an Mg^{2+}-resistant tonic I_{NMDA} in SNpc DA neurons in NR2D KO mice, and increased NR2D but not NR2B expression in the SNpc. In addition, genetic and pharmacological interventions with NR2D-containing eNMDARs attenuated MPTP-induced SNpc DA neurodegeneration and subsequent gait deficiency. These results show that the selective modulation of "recruited NR2D" could be an effective strategy for preventing and treating neurodegenerative diseases such as chemical-induced Parkinsonism. To the best of our knowledge, this is the first evidence that the state dependent recruitment of NR2D-containing eNMDARs can mediate an excitatory drive to facilitate neuronal death in the adult brain.

Cell type and stimulus specificity of extrasynaptic NR2D recruitment in the mature brain

Previously, we found that osmotic stimuli selectively recruited NR2D in supraoptic nucleus (SON) magnocellular neurosecretory

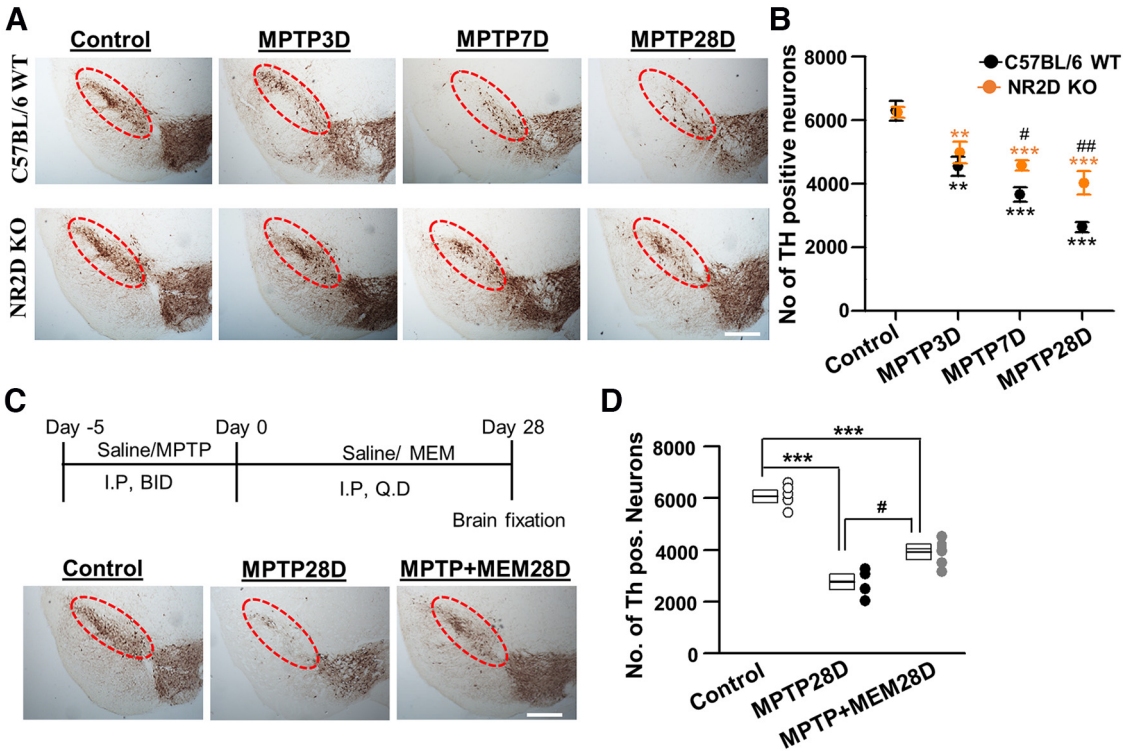

Figure 8. Effects of NR2D-KO and MEM on MPTP-induced SNpc DA neuronal death. ***A***, Representative images of TH-immunoreactive neurons in the SNpc from CTL and MPTP-injected WT and NR2D KO mice at 3, 7, and 28 d after MPTP injection. ***B***, Stereological quantification of TH-immunoreactive neurons in the SNpc demonstrated that a genetic NR2D intervention in mice protected dopaminergic neurons against MPTP toxicity (two-way RM-ANOVA, $F_{(1,40)} = 30.78$, $p = 0.002$; Bonferroni's *post hoc* test, #$p < 0.05$ and ##$p < 0.01$, WT vs KO and two-way RM-ANOVA, $F_{(1,40)} = 25.63$, $p = 0.002$; Bonferroni's *post hoc* test, **$p < 0.01$, and ***$p < 0.001$, WT-MPTP and KO-MPTP with respective controls, $n = 6$ mice in each group). ***C***, Representative images of TH-immunoreactive neurons in the SNpc from CTL, MPTP, and MPTP + MEM-treated WT mice. MEM treatment (10 mg/kg, i.p.; QD) was initiated on the first day after the complete dose of MPTP had been administered and continued until 28 d after MPTP injection (30 mg/kg, i.p.; BID), as shown by the timeline (top). ***D***, Stereological quantification of TH-immunoreactive neurons in the SNpc demonstrated that the comprehensive inhibition of extrasynaptic NMDA receptors protects dopaminergic neurons against MPTP toxicity (one-way ANOVA, $F_{(2,15)} = 75.70$, $p < 0.001$; Bonferroni's *post hoc* test, *$p < 0.05$, **$p < 0.001$, $n = 6$ mice in each group).

Table 3. Y-maze test performance by control and MPTP-injected WT and NR2D KO mice after 28 d of MPTP injection

	n	Numbers of arm entry	Alteration (%)
C57BL/6 WT			
Control	5	33.6 ± 3.18	65.65 ± 2.54
MPTP	5	30.6 ± 1.96	59.79 ± 1.43
NR2D KO			
Control	5	33.2 ± 3.06	64.51 ± 1.82
MPTP	5	29.8 ± 3.54	60.56 ± 3.52

cells (MNCs) that secreted the antidiuretic hormone vasopressin, leading to the generation of an Mg^{2+}-resistant tonic I_{NMDA}. This was not the case in neurons that secreted the reproductive hormone oxytocin (Neupane et al., 2021). Given that osmotic insult led to the selective recruitment of NR2D in vasopressin neurons but not oxytocin neurons, it is noteworthy that MPTP selectively generated Mg^{2+}-resistant tonic I_{NMDAs} in DA neurons but not in non-DA neurons in the present study. Combined with the fact that MPTP selectively targets DA neurons in the midbrain, these results support the idea that cell type-specific pathophysiological stimuli can recruit NR2D, leading to the generation of Mg^{2+}-resistant tonic I_{NMDA} in the mature brain (Neupane et al., 2021). MPP^+, which is a metabolite of MPTP, is taken into DA neurons by the dopamine transporter (DAT), where it exerts neurotoxic effects (Gainetdinov et al., 1997; Bezard et al., 1999). In previous studies, significantly more SNpc DA neurons than VTA DA neurons were found to express high levels of DAT (Reyes et al., 2013), and SNpc DA neurons also showed high vulnerability to MPTP compared with VTA DA neurons (Dauer and Przedborski, 2003). Incorporating these findings alongside our results showing more SNpc DA neurons than VTA DA neurons in MPTP-injected mice generated Mg^{2+}-resistant tonic I_{NMDA} (Fig. 4*C*) further support the notion that cell type-specific pathophysiological stimuli recruit extrasynaptic NR2D to generate Mg^{2+}-resistant tonic I_{NMDA} in the mature brain.

Given that MPTP generated Mg^{2+}-resistant tonic I_{NMDA} in DA neurons but not in non-DA neurons in the present study, it is noteworthy that NR2D mRNA is highly expressed in SNpc neurons (Standaert et al., 1994; Counihan et al., 1998), especially TH-positive DA neurons (Counihan et al., 1998). Similarly, osmotic insult led to the selective recruitment of NR2D in vasopressin neurons but not oxytocin neurons, and VP neurons express higher levels of NR2D mRNA than OT neurons in the SON (Al-Ghoul et al., 1997). Overall, these results suggest that extrasynaptic NR2D recruitment is a common component of cell type-specific pathophysiology in NR2D mRNA-enriched neurons in the mature brain.

NMDAR-containing NR2D subunits are involved in synaptic events such as altered EPSC amplitudes and/or decay times in an activity-dependent manner during postnatal development (Clark and Cull-Candy, 2002; Harney et al., 2008). In SNpc DA neurons, sEPSCs mediated by NR2D-containing receptors may appear in the immature [postnatal day (P)4–P10], but not young, adult brain (P30–P50; Jones and Gibb, 2005; Pearlstein et al., 2015). Combined with the finding that NR2D KO can abolish Mg^{2+}-resistant tonic I_{NMDA} according to cell type-specific stimuli (Fig. 3 in the present study; Neupane et al., 2021), these results indicate that extrasynaptic recruitment of NR2D-containing receptors is

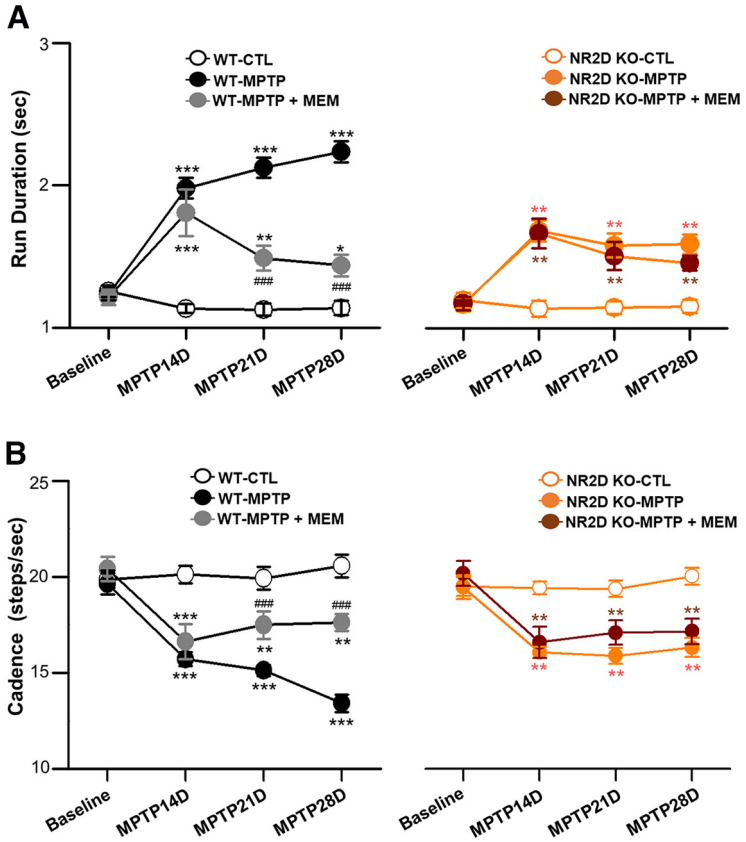

Figure 9. Effects of NR2D-KO and MEM on MPTP-induced gait abnormalities in mice. ***A***, Run duration (s) of CTL, MPTP and MPTP + MEM group from WT (right) and NR2D KO mice (left) before MPTP injection (baseline) and 14, 21, and 28 d after MPTP injection; (WT mice: one-way ANOVA, $F_{(2,208)} = 45.38$, $p < 0.001$; Bonferroni's *post hoc* test, ###$p < 0.001$, MPTP vs MPTP + MEM and *$p < 0.05$, **$p < 0.01$, and ***$p < 0.001$, WT-MPTP and MPTP + MEM with their respective control groups, $n = 10$–25 mice in each group) and (NR2D KO mice: two-way ANOVA, $F_{(2,164)} = 11.39$; Bonferroni's *post hoc* test, $p > 0.90$, KO-MPTP vs KO-MPTP + MEM and *$p < 0.05$, **$p < 0.01$, and ***$p < 0.001$, KO-MPTP and MPTP + MEM with their respective control groups, $n = 8$–18 mice in each group). ***B***, Cadence (steps/s) of CTL, MPTP, and MPTP + MEM group from WT (right) and NR2D KO (left) mice before MPTP injection (baseline) and 14, 21, and 28 d after MPTP injection; (WT mice: one-way ANOVA, $F_{(2,208)} = 24.93$, $p < 0.001$; Bonferroni's *post hoc* test, ###$p < 0.001$, MPTP vs MPTP + MEM and *$p < 0.05$, **$p < 0.01$, and ***$p < 0.001$, WT-MPTP and MPTP + MEM with their respective control groups, $n = 10$–25 mice in each group) and (NR2D KO mice: one-way ANOVA, $F_{(2,164)} = 11.84$; Bonferroni's *post hoc* test, $p > 0.90$, KO-MPTP vs KO-MPTP + MEM and *$p < 0.05$, **$p < 0.01$, and ***$p < 0.001$, KO-MPTP and MPTP + MEM with their respective control groups, $n = 8$–18 mice in each group).

Table 4. Effect of memantine treatment in stride length (cm) and stance duration (s) on 28 d after saline or MPTP injection in C57BL/6-WT mice

	RF	RH	LF	LH
Stride length (cm)				
CTL	8.152 ± 0.187	8.016 ± 0.183	8.160 ± 0.181	8.159 ± 0.175
MPTP	6.168 ± 0.173***	5.98 ± 0.212***	6.239 ± 0.172***	6.137 ± 0.179***
MPTP-MEM	7.400 ± 0.154	7.377 ± 0.163	7.254 ± 0.166	7.341 ± 0.165
MPTP vs MPTP-MEM	##	###	##	###
Stance (s)				
CTL	0.089 ± 0.004	0.084 ± 0.003	0.090 ± 0.004	0.084 ± 0.003
MPTP	0.168 ± 0.004***	0.158 ± 0.007***	0.158 ± 0.006***	0.165 ± 0.003***
MPTP	0.105 ± 0.006	0.101 ± 0.005	0.104 ± 0.005	0.100 ± 0.007
MPTP vs MPTP-MEM	###	###	###	###

CTL: C57BL/6-WT-saline injection; MPTP: C57BL/6-WT-MPTP injection; MPTP-MEM: C57BL/6-WT-MPTP injection + memantine injection.
***$p < 0.001$, compared with respective control, Bonferroni's *post hoc* test following one-way ANOVA.
##$p < 0.01$, ###$p < 0.001$, compared with MPTP, Bonferroni's *post hoc* test following one-way ANOVA.

essential for the generation of Mg^{2+}-resistant tonic I_{NMDA} in the mature brain. However, given that pathophysiological stimuli alter the subsynaptic location of the extrasynaptic receptor subunit (Chen et al., 2018), we cannot completely exclude the possibility that synaptic NR2D contributes to tonic I_{NMDA} in the mature brain. Indeed, NMDAR antagonism marginally shifted $I_{holding}$ in some recordings in the present study. However, ambient glutamate failed to generate Mg^{2+}-resistant tonic I_{NMDA} in normal DA neurons (Fig. 7*A*–*C*) or VP neurons (Neupane et al., 2021). These results suggest that synaptic NMDARs containing NR2D mediate sEPSCs in the early postnatal period, whereas the pathophysiological recruitment of their extrasynaptic counterpart generates Mg^{2+}-resistant tonic I_{NMDA} in the mature brain.

Overall, our results expand our understanding of state-dependent NR2D plasticity. Specifically, we found that cell type-specific pathophysiological stimuli can recruit NR2D in extrasynaptic regions, leading to the generation of Mg^{2+}-resistant tonic I_{NMDA} in the mature brain.

Table 5. Effect of memantine treatment in stride length (cm) and stance duration (s) on 28 d after saline or MPTP injection in NR2D-KO mice

	RF	RH	LF	LH
Stride length (cm)				
KO-CTL	8.308 ± 0.211	8.349 ± 0.185	8.252 ± 0.218	8.229 ± 0.207
KO-MPTP	7.321 ± 0.151***	7.246 ± 0.169**	7.150 ± 0.185**	7.274 ± 0.129***
KO-MPTP-MEM	7.250 ± 0.210	7.032 ± 0.290	7.272 ± 0.197	7.371 ± 0.190
MPTP vs MPTP-MEM	ns	ns	ns	ns
Stance (s)				
KO-CTL	0.088 ± 0.002	0.087 ± 0.002	0.091 ± 0.002	0.095 ± 0.003
KO-MPTP	0.122 ± 0.005***	0.124 ± 0.004***	0.127 ± 0.005***	0.127 ± 0.006**
KO-MPTP-MEM	0.116 ± 0.005	0.116 ± 0.005	0.125 ± 0.006	0.117 ± 0.008
MPTP vs MPTP-MEM	ns	ns	ns	ns

KO-CTL: NR2D KO-saline injection; KO- MPTP: NR2D KO-MPTP injection; KO-MPTP-MEM: NR2D KO-MPTP injection + memantine injection.
**$p < 0.01$, ***$p < 0.001$, compared with respective control, Bonferroni's *post hoc* test following one-way ANOVA.
ns = not significant, compared with MPTP, Bonferroni's *post hoc* test following one-way ANOVA.

MPTP recruits NR2D-NR1 heterodimeric receptors in SNpc DA neurons

eNMDARs in many CNS regions are predominantly composed of NR2B and/or NR2D subunits forming heterodimeric (NR2B-NR1 or NR2D-NR1) or heterotrimeric (NR2B/NR2D-NR1) structures (Sheng et al., 1994; Momiyama et al., 1996; Dunah et al., 1998; Misra et al., 2000; Momiyama, 2000; Brickley et al., 2003). Combined with the fact that NR2D subunits are expressed in extrasynaptic sites (Lozovaya et al., 2004), NR2D-containing NMDARs are ideal candidates for the mediation of Mg^{2+}-resistant tonic I_{NMDA} given their low Mg^{2+} sensitivity (Monyer et al., 1994; Kuner and Schoepfer, 1996; Momiyama et al., 1996; Huang and Gibb, 2014), slow rate of deactivation (Vicini et al., 1998; Wyllie et al., 1998), and high glutamate sensitivity (Erreger et al., 2007).

In addition to biophysical properties, the pharmacological properties of NMDARs are important for understanding the stoichiometric composition of NMDAR subunits. For example, ifenprodil blocks both heterodimeric NR2B-NR1 receptors and heterotrimeric NR2B/NR2D-NR1 receptors (Brothwell et al., 2008). Thus, our finding that Mg^{2+}-resistant tonic I_{NMDA} was insensitive to ifenprodil indicates that MPTP recruits NR2D-NR1 homodimeric receptors rather than NR2B/NR2D-NR1 heterotrimers that mediate Mg^{2+}-resistant tonic I_{NMDA} in neurons. This idea is in agreement with our finding that MPTP intoxication selectively increased NR2D over NR2B expression in the midbrain (Fig. 4). Similarly, we concluded in a previous study that osmotic stimuli recruited eNMDARs composed of NR2D-NR1 homodimeric receptors in SON MNCs (Neupane et al., 2021), where these stimuli generated Mg^{2+}-resistant tonic I_{NMDAs} that were insensitive to ifenprodil. Overall, our results suggest that cell type-specific stimuli can recruit homodimeric NR2D-NR1 eNMDARs that generate tonic I_{NMDA} DA neurons in the mature brain.

NR2D-containing eNMDARs trigger DA neuronal death

Since the discovery of glutamate (Choi, 1987; Choi et al., 1987) and NMDA-induced cell death (Choi et al., 1988; Tymianski et al., 1993), NMDARs have been studied intensively to characterize their role in neurotoxicity (in addition to their previously defined role in synaptic transmission). This excitotoxicity is caused solely by eNMDARs composed of NR2B subunits (Jourdain et al., 2007; Nicolai et al., 2010; Tu et al., 2010; Tang et al., 2018) or NR2D subunits (Jullienne et al., 2011; Bai et al., 2013), which cause intracellular Ca^{2+} overload. By contrast, the activation of synaptic NMDARs promotes neuronal survival and synaptic plasticity, as in hippocampal neurons (Wroge et al., 2012). This idea is supported by our present finding that eNMDAR-containing NR2D subunits generate an Mg^{2+}-resistant tonic I_{NMDA}, thus triggering cell death in toxin-based parkinsonian models.

Table 6. I_{PPDA} amplitude (pA), cell capacitance (c_m), and current density (pA/pF) in nondepolarized SON MNCs and SNpc DA neurons

	SNpc DA neurons		SON-MNCS VP neurons	
	CTL	MPTP	CTL	SL
IPPDA(pA)	0.53 ± 0.24	6.44 ± 0.53	0.79 ± 0.25	7.07 ± 1.20
Cell capacitance, cm (pF)	57.76 ± 4.19	53.97 ± 6.07	108 ± 10.07	131.61 ± 19.59
IPPDA current density (pA/pF)	0.009 ± 0.005	0.11 ± 0.01	0.008 ± 0.001	0.06 ± 0.01

I_{PPDA}: PPDA sensitive tonic NMDA current.
SON-MNCS VP neurons; vasopressin releasing magnocellular neurosecretory cells (MNCs) from hypothalamic supraoptic nucleus (SON).
SL: 7-d salt loading model mice (for details, see Neupane et al., 2021).

However, we previously suggested that Mg^{2+}-resistant tonic I_{NMDA} (mediated by NR2D-containing eNMDARs) would be an ideal candidate for enhancing neuronal excitability with less excitotoxicity in SON MNCs (Neupane et al., 2021). As mentioned above, this excitotoxicity is caused by eNMDAR activity leading to intracellular Ca^{2+} overload. This apparent discrepancy may be resolved by considering that Ca^{2+} overload elicited by extrasynaptic NR2D recruitment is sufficient to trigger pro-death signaling in SNpc DA neurons but not in magnocellular neurons, which is supported by our finding that the current density of the Mg^{2+}-resistant tonic I_{NMDA} was significantly larger in MPTP-treated DA neurons than in salt-loaded VP neurons (Table 6), although the mean amplitude of the current was similar in both neuron types (VP neurons, 7.07 ± 1.20 pA; SNpc DA neurons, 6.44 ± 0.53 pA).

Although eNMDARs mediate Ca^{2+} influx-provoking pro-death signaling, such as mitochondria dysfunction, in some neurons (Kaufman et al., 2012), the activation of eNMDAR alone is not neurotoxic (X. Zhou et al., 2013). Interestingly, the endoplasmic reticulum takes up, but does not release, Ca^{2+} in response to NMDAR activation in SON MNCs (M. Zhang and Stern, 2017), suggesting that the characteristic eNMDAR-ER coupling prevents Ca^{2+} overload in SON MNCs. In PD models, pace making in SNpc but not in VTA is accompanied by calcium influx through L-type calcium channel, $Ca_V1.3$ contributing to increased intracellular calcium and hence to cell death (Surmeier et al., 2010; Verma and Ravindranath, 2019). Indeed, dysregulation in calcium homeostasis could potentially account for the selective vulnerability of SNpc and VTA DA neurons to MPTP (Mosharov et al., 2009; Surmeier et al., 2011; Surmeier and Schumacker, 2013). This may explain that, even with the similar

current density (Tables 4, 5), Mg^{2+}-resistant tonic I_{NMDA} trigger MPTP-induced DA neuronal death in SNpc but not in VTA (Fig. 8). Overall, these results supported the idea that the activation of eNMDARs generating Mg^{2+}-resistant tonic I_{NMDA} alone may not be excitotoxic. However, combined with the finding that the current density of the Mg^{2+}-resistant tonic I_{NMDA} was low in salt-loaded VP neurons and that the proportion of DA neurons generating Mg^{2+}-resistant tonic I_{NMDA} is lower in VTA than in SNpc (Fig. 4*C*), we cannot exclude the possibility that extrasynaptic NR2D generally triggers neuronal loss. Future studies are warranted to determine whether the tonic activation of NR2D-containing eNMDARs inevitably contributes to neuronal death in various pathophysiological brain processes.

Functional significance of extrasynaptic NR2D recruitment in DA neuronal death

The altered expression and/or composition of NMDARs is an underlying molecular mechanism in neurologic disorders ranging from acute synaptic overdrive to chronic neurodegeneration. In the present study, we demonstrated that state-dependent recruitment of extrasynaptic NR2D critically upregulates excitatory glutamatergic input even in nondepolarized neurons, which may trigger excitotoxicity in SNpc DA neurons. Combined with the finding that Mg^{2+}-resistant tonic I_{NMDA} increased neuronal excitability and enhanced antidiuretic hormone release in magnocellular neurons (Neupane et al., 2021), our results indicate that extrasynaptic NR2D recruitment in the mature brain is a form of state-dependent NMDAR plasticity that is generally involved in both neuronal excitability and excitotoxicity. Future studies are warranted to establish whether extrasynaptic NR2D recruitment is a common component of neuronal overdrive and/or neurodegeneration in various brain regions and neurologic diseases and vice versa.

SNpc DA neuronal loss plays significant role in precipitating motor dysfunction (Damier et al., 1999; Michel et al., 2016), whereas VTA DA neuronal loss has been implicated in nonmotor manifestations (Narayanan et al., 2013; Friedman et al., 2014; H. Wang et al., 2023). Given that VTA DA neurons demonstrate a higher degree of resistance to degeneration than SNpc DA neurons in PD (Dauer and Przedborski, 2003), it is notable that MPTP caused gait deficits without significant nonmotor impairments in both WT and NR2D KO mice in the present study. Our results showing that the proportion of DA neurons generating Mg^{2+}-resistant tonic I_{NMDA} is lower in VTA than in SNpc (Fig. 4*C*) is also consistent with the notion that VTA DA neurons would be more resistant to NR2D-mediated cell death. However, considerable molecular and electrophysiological heterogeneity among the DA neurons makes it challenging to elucidate the molecular mechanisms underlying DA vulnerability in PD. Given that we used systemic NR2D KO animals in the present study, future studies involving cell type-specific NR2D gene manipulation may improve our understanding of the functional significance of extrasynaptic NR2D in midbrain DA circuits and neuronal death in DA and/or SON MNCs.

Excessive glutamate levels have been detected in pathologic conditions such as PD (Conn et al., 2005; Sebastianutto and Cenci, 2018), which results in the abnormal stimulation of NMDA receptors, in turn triggering a cascade of excitation-mediated neuronal damage. Combined with the fact that NMDARs containing NR2D subunits exhibit higher glutamate sensitivity, the Mg^{2+}-resistant tonic I_{NMDA} generated by NR2D-containing receptors could make them ideal mediators of glutamate-induced excitotoxicity, even at physiological glutamate concentrations if the current density exceeds the threshold. In addition, MEM treatment has been found to reduce akinesia and rigidity in animal models (Kucheryanu and Kryzhanovskii, 2000) and improve axial signs in human patients (Moreau et al., 2013). In the current study, we found that it improved abnormal gait (Fig. 9). Given that competitive NMDAR antagonists failed in clinical trials because of serious adverse effects such as cognitive changes and sedation, our results shed light on a new path targeting the state-dependent recruitment of homodimeric NR2D-NR1 eNMDARs in the mature brain as a potential target for neuroprotective strategies.

References

Al-Ghoul WM, Meeker RB, Greenwood RS (1997) Differential expression of five N-methyl-D-aspartate receptor subunit mRNAs in vasopressin and oxytocin neuroendocrine cells. Brain Res Mol Brain Res 44:262–272.

Bai N, Hayashi H, Aida T, Namekata K, Harada T, Mishina M, Tanaka K (2013) Dock3 interaction with a glutamate-receptor NR2D subunit protects neurons from excitotoxicity. Mol Brain 6:22.

Bezard E, Gross CE, Fournier MC, Dovero S, Bloch B, Jaber M (1999) Absence of MPTP-induced neuronal death in mice lacking the dopamine transporter. Exp Neurol 155:268–273.

Bissonette GB, Roesch MR (2016) Development and function of the midbrain dopamine system: what we know and what we need to. Genes Brain Behav 15:62–73.

Boix J, von Hieber D, Connor B (2018) Gait analysis for early detection of motor symptoms in the 6-OHDA rat model of Parkinson's disease. Front Behav Neurosci 12:39.

Brichta L, Greengard P, Flajolet M (2013) Advances in the pharmacological treatment of Parkinson's disease: targeting neurotransmitter systems. Trends Neurosci 36:543–554.

Brickley SG, Misra C, Mok MH, Mishina M, Cull-Candy SG (2003) NR2B and NR2D subunits coassemble in cerebellar Golgi cells to form a distinct NMDA receptor subtype restricted to extrasynaptic sites. J Neurosci 23:4958–4966.

Brothwell SL, Barber JL, Monaghan DT, Jane DE, Gibb AJ, Jones S (2008) NR2B- and NR2D-containing synaptic NMDA receptors in developing rat substantia nigra pars compacta dopaminergic neurones. J Physiol 586:739–750.

Castelli V, d'Angelo M, Lombardi F, Alfonsetti M, Antonosante A, Catanesi M, Benedetti E, Palumbo P, Cifone MG, Giordano A, Desideri G, Cimini A (2020) Effects of the probiotic formulation SLAB51 in in vitro and in vivo Parkinson's disease models. Aging (Albany NY) 12:4641–4659.

Chen H, Tang AH, Blanpied TA (2018) Subsynaptic spatial organization as a regulator of synaptic strength and plasticity. Curr Opin Neurobiol 51:147–153.

Chenard BL, Menniti FS (1999) Antagonists selective for NMDA receptors containing the NR2B subunit. Curr Pharm Des 5:381–404.

Choi DW (1987) Ionic dependence of glutamate neurotoxicity. J Neurosci 7:369–379.

Choi DW, Maulucci-Gedde M, Kriegstein AR (1987) Glutamate neurotoxicity in cortical cell culture. J Neurosci 7:357–368.

Choi DW, Koh JY, Peters S (1988) Pharmacology of glutamate neurotoxicity in cortical cell culture: attenuation by NMDA antagonists. J Neurosci 8:185–196.

Chung YC, Bok E, Huh SH, Park JY, Yoon SH, Kim SR, Kim YS, Maeng S, Park SH, Jin BK (2011) Cannabinoid receptor type 1 protects nigrostriatal dopaminergic neurons against MPTP neurotoxicity by inhibiting microglial activation. J Immunol 187:6508–6517.

Clark BA, Cull-Candy SG (2002) Activity-dependent recruitment of extrasynaptic NMDA receptor activation at an AMPA receptor-only synapse. J Neurosci 22:4428–4436.

Conn PJ, Battaglia G, Marino MJ, Nicoletti F (2005) Metabotropic glutamate receptors in the basal ganglia motor circuit. Nat Rev Neurosci 6:787–798.

Counihan TJ, Landwehrmeyer GB, Standaert DG, Kosinski CM, Scherzer CR, Daggett LP, Veliçelebi G, Young AB, Penney JB Jr (1998) Expression of N-methyl-D-aspartate receptor subunit mRNA in the human brain: mesencephalic dopaminergic neurons. J Comp Neurol 390:91–101.

Da Cunha C, Wietzikoski S, Wietzikoski EC, Miyoshi E, Ferro MM, Anselmo-Franci JA, Canteras NS (2003) Evidence for the substantia nigra

pars compacta as an essential component of a memory system independent of the hippocampal memory system. Neurobiol Learn Mem 79:236–242.

Damier P, Hirsch EC, Agid Y, Graybiel AM (1999) The substantia nigra of the human brain. II. Patterns of loss of dopamine-containing neurons in Parkinson's disease. Brain 122:1437–1448.

Dauer W, Przedborski S (2003) Parkinson's disease: mechanisms and models. Neuron 39:889–909.

Deumens R, Koopmans GC, Honig WM, Hamers FP, Maquet V, Jérôme R, Steinbusch HW, Joosten EA (2006) Olfactory ensheathing cells, olfactory nerve fibroblasts and biomatrices to promote long-distance axon regrowth and functional recovery in the dorsally hemisected adult rat spinal cord. Exp Neurol 200:89–103.

Dunah AW, Yasuda RP, Wang YH, Luo J, Dávila-García M, Gbadegesin M, Vicini S, Wolfe BB (1996) Regional and ontogenic expression of the NMDA receptor subunit NR2D protein in rat brain using a subunit-specific antibody. J Neurochem 67:2335–2345.

Dunah AW, Luo J, Wang YH, Yasuda RP, Wolfe BB (1998) Subunit composition of N-methyl-D-aspartate receptors in the central nervous system that contain the NR2D subunit. Mol Pharmacol 53:429–437.

Erreger K, Geballe MT, Kristensen A, Chen PE, Hansen KB, Lee CJ, Yuan H, Le P, Lyuboslavsky PN, Micale N, Jørgensen L, Clausen RP, Wyllie DJ, Snyder JP, Traynelis SF (2007) Subunit-specific agonist activity at NR2A-, NR2B-, NR2C-, and NR2D-containing N-methyl-D-aspartate glutamate receptors. Mol Pharmacol 72:907–920.

Feng B, Tse HW, Skifter DA, Morley R, Jane DE, Monaghan DT (2004) Structure-activity analysis of a novel NR2C/NR2D-preferring NMDA receptor antagonist: 1-(phenanthrene-2-carbonyl) piperazine-2,3-dicarboxylic acid. Br J Pharmacol 141:508–516.

Ferguson SA, Law CD, Sarkar S (2015) Chronic MPTP treatment produces hyperactivity in male mice which is not alleviated by concurrent trehalose treatment. Behav Brain Res 292:68–78.

Friedman AK, Walsh JJ, Juarez B, Ku SM, Chaudhury D, Wang J, Li X, Dietz DM, Pan N, Vialou VF, Neve RL, Yue Z, Han MH (2014) Enhancing depression mechanisms in midbrain dopamine neurons achieves homeostatic resilience. Science 344:313–319.

Gainetdinov RR, Fumagalli F, Jones SR, Caron MG (1997) Dopamine transporter is required for in vivo MPTP neurotoxicity: evidence from mice lacking the transporter. J Neurochem 69:1322–1325.

Han NR, Kim YK, Ahn S, Hwang TY, Lee H, Park HJ (2020) A comprehensive phenotype of non-motor impairments and distribution of alpha-synuclein deposition in parkinsonism-induced mice by a combination injection of MPTP and probenecid. Front Aging Neurosci 12:599045.

Hardingham GE, Bading H (2010) Synaptic versus extrasynaptic NMDA receptor signalling: implications for neurodegenerative disorders. Nat Rev Neurosci 11:682–696.

Harney SC, Jane DE, Anwyl R (2008) Extrasynaptic NR2D-containing NMDARs are recruited to the synapse during LTP of NMDAR-EPSCs. J Neurosci 28:11685–11694.

Huang Z, Gibb AJ (2014) Mg^{2+} block properties of triheteromeric GluN1-GluN2B-GluN2D NMDA receptors on neonatal rat substantia nigra pars compacta dopaminergic neurones. J Physiol 592:2059–2078.

Ikeda K, Araki K, Takayama C, Inoue Y, Yagi T, Aizawa S, Mishina M (1995) Reduced spontaneous activity of mice defective in the epsilon 4 subunit of the NMDA receptor channel. Brain Res Mol Brain Res 33:61–71.

Jackson-Lewis V, Przedborski S (2007) Protocol for the MPTP mouse model of Parkinson's disease. Nat Protoc 2:141–151.

Jones S, Gibb AJ (2005) Functional NR2B- and NR2D-containing NMDA receptor channels in rat substantia nigra dopaminergic neurones. J Physiol 569:209–221.

Jourdain P, Bergersen LH, Bhaukaurally K, Bezzi P, Santello M, Domercq M, Matute C, Tonello F, Gundersen V, Volterra A (2007) Glutamate exocytosis from astrocytes controls synaptic strength. Nat Neurosci 10:331–339.

Jullienne A, Montagne A, Orset C, Lesept F, Jane DE, Monaghan DT, Maubert E, Vivien D, Ali C (2011) Selective inhibition of GluN2D-containing N-methyl-D-aspartate receptors prevents tissue plasminogen activator-promoted neurotoxicity both in vitro and in vivo. Mol Neurodegener 6:68.

Kaufman AM, Milnerwood AJ, Sepers MD, Coquinco A, She K, Wang L, Lee H, Craig AM, Cynader M, Raymond LA (2012) Opposing roles of synaptic and extrasynaptic NMDA receptor signaling in cocultured striatal and cortical neurons. J Neurosci 32:3992–4003.

Koopmans GC, Deumens R, Brook G, Gerver J, Honig WM, Hamers FP, Joosten EA (2007) Strain and locomotor speed affect over-ground locomotion in intact rats. Physiol Behav 92:993–1001.

Krashia P, Martini A, Nobili A, Aversa D, D'Amelio M, Berretta N, Guatteo E, Mercuri NB (2017) On the properties of identified dopaminergic neurons in the mouse substantia nigra and ventral tegmental area. Eur J Neurosci 45:92–105.

Kucheryanu VG, Kryzhanovskii GN (2000) Effect of glutamate and antagonists of N-methyl-D-aspartate receptors on experimental parkinsonian syndrome in rats. Bull Exp Biol Med 130:629–632.

Kuner T, Schoepfer R (1996) Multiple structural elements determine subunit specificity of Mg^{2+} block in NMDA receptor channels. J Neurosci 16:3549–3558.

Liu Q, Wong-Riley MT (2010) Postnatal development of N-methyl-D-aspartate receptor subunits 2A, 2B, 2C, 2D, and 3B immunoreactivity in brain stem respiratory nuclei of the rat. Neuroscience 171:637–654.

Liu Y, Wong TP, Aarts M, Rooyakkers A, Liu L, Lai TW, Wu DC, Lu J, Tymianski M, Craig AM, Wang YT (2007) NMDA receptor subunits have differential roles in mediating excitotoxic neuronal death both in vitro and in vivo. J Neurosci 27:2846–2857.

Lozovaya NA, Grebenyuk SE, Tsintsadze T, Feng B, Monaghan DT, Krishtal OA (2004) Extrasynaptic NR2B and NR2D subunits of NMDA receptors shape 'superslow' afterburst EPSC in rat hippocampus. J Physiol 558:451–463.

Michel PP, Hirsch EC, Hunot S (2016) Understanding dopaminergic cell death pathways in Parkinson disease. Neuron 90:675–691.

Milnerwood AJ, Kaufman AM, Sepers MD, Gladding CM, Zhang L, Wang L, Fan J, Coquinco A, Qiao JY, Lee H, Wang YT, Cynader M, Raymond LA (2012) Mitigation of augmented extrasynaptic NMDAR signaling and apoptosis in cortico-striatal co-cultures from Huntington's disease mice. Neurobiol Dis 48:40–51.

Misra C, Brickley SG, Farrant M, Cull-Candy SG (2000) Identification of subunits contributing to synaptic and extrasynaptic NMDA receptors in Golgi cells of the rat cerebellum. J Physiol 524:147–162.

Momiyama A (2000) Distinct synaptic and extrasynaptic NMDA receptors identified in dorsal horn neurones of the adult rat spinal cord. J Physiol 523:621–628.

Momiyama A, Feldmeyer D, Cull-Candy SG (1996) Identification of a native low-conductance NMDA channel with reduced sensitivity to Mg^{2+} in rat central neurones. J Physiol 494:479–492.

Monyer H, Burnashev N, Laurie DJ, Sakmann B, Seeburg PH (1994) Developmental and regional expression in the rat brain and functional properties of four NMDA receptors. Neuron 12:529–540.

Moreau C, Delval A, Tiffreau V, Defebvre L, Dujardin K, Duhamel A, Petyt G, Hossein-Foucher C, Blum D, Sablonnière B, Schraen S, Allorge D, Destée A, Bordet R, Devos D (2013) Memantine for axial signs in Parkinson's disease: a randomised, double-blind, placebo-controlled pilot study. J Neurol Neurosurg Psychiatry 84:552–555.

Mosharov EV, Larsen KE, Kanter E, Phillips KA, Wilson K, Schmitz Y, Krantz DE, Kobayashi K, Edwards RH, Sulzer D (2009) Interplay between cytosolic dopamine, calcium, and alpha-synuclein causes selective death of substantia nigra neurons. Neuron 62:218–229.

Narayanan NS, Rodnitzky RL, Uc EY (2013) Prefrontal dopamine signaling and cognitive symptoms of Parkinson's disease. Rev Neurosci 24:267–278.

Neupane C, Sharma R, Pai YH, Lee SY, Jeon BH, Kim HW, Stern JE, Park JB (2021) High salt intake recruits tonic activation of NR2D subunit-containing extrasynaptic NMDARs in vasopressin neurons. J Neurosci 41:1145–1156.

Nicolai J, Burbassi S, Rubin J, Meucci O (2010) CXCL12 inhibits expression of the NMDA receptor's NR2B subunit through a histone deacetylase-dependent pathway contributing to neuronal survival. Cell Death Dis 1:e33.

Otomo K, Perkins J, Kulkarni A, Stojanovic S, Roeper J, Paladini CA (2020) In vivo patch-clamp recordings reveal distinct subthreshold signatures and threshold dynamics of midbrain dopamine neurons. Nat Commun 11:6286.

Paoletti P, Bellone C, Zhou Q (2013) NMDA receptor subunit diversity: impact on receptor properties, synaptic plasticity and disease. Nat Rev Neurosci 14:383–400.

Park SE, Neupane C, Noh C, Sharma R, Shin HJ, Pham TL, Lee GS, Park KD, Lee CJ, Kang DW, Lee SY, Kim HW, Park JB (2022) Antiallodynic effects of KDS2010, a novel MAO-B inhibitor, via ROS-GABA inhibitory transmission in a paclitaxel-induced tactile hypersensitivity model. Mol Brain 15:41.

Pearlstein E, Gouty-Colomer LA, Michel FJ, Cloarec R, Hammond C (2015) Glutamatergic synaptic currents of nigral dopaminergic neurons follow a postnatal developmental sequence. Front Cell Neurosci 9:210.

Reyes S, Fu Y, Double KL, Cottam V, Thompson LH, Kirik D, Paxinos G, Watson C, Cooper HM, Halliday GM (2013) Trophic factors differentiate dopamine neurons vulnerable to Parkinson's disease. Neurobiol Aging 34:873–886.

Sawamoto K, Nakao N, Kobayashi K, Matsushita N, Takahashi H, Kakishita K, Yamamoto A, Yoshizaki T, Terashima T, Murakami F, Itakura T, Okano H (2001) Visualization, direct isolation, and transplantation of midbrain dopaminergic neurons. Proc Natl Acad Sci U S A 98:6423–6428.

Sebastianutto I, Cenci MA (2018) mGlu receptors in the treatment of Parkinson's disease and L-DOPA-induced dyskinesia. Curr Opin Pharmacol 38:81–89.

Sheng M, Cummings J, Roldan LA, Jan YN, Jan LY (1994) Changing subunit composition of heteromeric NMDA receptors during development of rat cortex. Nature 368:144–147.

Standaert DG, Testa CM, Young AB, Penney JB Jr (1994) Organization of N-methyl-D-aspartate glutamate receptor gene expression in the basal ganglia of the rat. J Comp Neurol 343:1–16.

Stark DT, Bazan NG (2011) Synaptic and extrasynaptic NMDA receptors differentially modulate neuronal cyclooxygenase-2 function, lipid peroxidation, and neuroprotection. J Neurosci 31:13710–13721.

Stott SR, Hayat S, Carnwath T, Garas S, Sleeman JP, Barker RA (2017) CD24 expression does not affect dopamine neuronal survival in a mouse model of Parkinson's disease. PLoS One 12:e0171748.

Stott SRW, Barker RA (2014) Time course of dopamine neuron loss and glial response in the 6-OHDA striatal mouse model of Parkinson's disease. Eur J Neurosci 39:1042–1056.

Surmeier DJ, Schumacker PT (2013) Calcium, bioenergetics, and neuronal vulnerability in Parkinson's disease. J Biol Chem 288:10736–10741.

Surmeier DJ, Guzman JN, Sanchez-Padilla J (2010) Calcium, cellular aging, and selective neuronal vulnerability in Parkinson's disease. Cell Calcium 47:175–182.

Surmeier DJ, Guzman JN, Sanchez-Padilla J, Schumacker PT (2011) The role of calcium and mitochondrial oxidant stress in the loss of substantia nigra pars compacta dopaminergic neurons in Parkinson's disease. Neuroscience 198:221–231.

Tang N, Wu J, Zhu H, Yan H, Guo Y, Cai Y, Yan H, Shi Y, Shu S, Pei L, Lu Y (2018) Genetic mutation of GluN2B protects brain cells against stroke damages. Mol Neurobiol 55:2979–2990.

Tu W, Xu X, Peng L, Zhong X, Zhang W, Soundarapandian MM, Balel C, Wang M, Jia N, Zhang W, Lew F, Chan SL, Chen Y, Lu Y (2010) DAPK1 interaction with NMDA receptor NR2B subunits mediates brain damage in stroke. Cell 140:222–234.

Tymianski M, Charlton MP, Carlen PL, Tator CH (1993) Source specificity of early calcium neurotoxicity in cultured embryonic spinal neurons. J Neurosci 13:2085–2104.

Verma A, Ravindranath V (2019) Ca(V)1.3 L-type calcium channels increase the vulnerability of substantia nigra dopaminergic neurons in MPTP mouse model of Parkinson's disease. Front Aging Neurosci 11:382.

Vicini S, Wang JF, Li JH, Zhu WJ, Wang YH, Luo JH, Wolfe BB, Grayson DR (1998) Functional and pharmacological differences between recombinant N-methyl-D-aspartate receptors. J Neurophysiol 79:555–566.

Wang H, Cui W, Chen W, Liu F, Dong Z, Xing G, Luo B, Gao N, Zou WJ, Zhao K, Zhang H, Ren X, Yu Z, Robinson HL, Liu Z, Xiong WC, Mei L (2023) The laterodorsal tegmentum-ventral tegmental area circuit controls depression-like behaviors by activating ErbB4 in DA neurons. Mol Psychiatry 28:1027–1045.

Wang XH, Lu G, Hu X, Tsang KS, Kwong WH, Wu FX, Meng HW, Jiang S, Liu SW, Ng HK, Poon WS (2012) Quantitative assessment of gait and neurochemical correlation in a classical murine model of Parkinson's disease. BMC Neurosci 13:142.

Watanabe Y, Gould E, McEwen BS (1992) Stress induces atrophy of apical dendrites of hippocampal CA3 pyramidal neurons. Brain Res 588:341–345.

Wenzel A, Villa M, Mohler H, Benke D (1996) Developmental and regional expression of NMDA receptor subtypes containing the NR2D subunit in rat brain. J Neurochem 66:1240–1248.

White RB, Thomas MG (2012) Moving beyond tyrosine hydroxylase to define dopaminergic neurons for use in cell replacement therapies for Parkinson's disease. CNS Neurol Disord Drug Targets 11:340–349.

Wild AR, Bollands M, Morris PG, Jones S (2015) Mechanisms regulating spill-over of synaptic glutamate to extrasynaptic NMDA receptors in mouse substantia nigra dopaminergic neurons. Eur J Neurosci 42:2633–2643.

Wroge CM, Hogins J, Eisenman L, Mennerick S (2012) Synaptic NMDA receptors mediate hypoxic excitotoxic death. J Neurosci 32:6732–6742.

Wu YN, Johnson SW (2015) Memantine selectively blocks extrasynaptic NMDA receptors in rat substantia nigra dopamine neurons. Brain Res 1603:1–7.

Wyllie DJ, Béhé P, Colquhoun D (1998) Single-channel activations and concentration jumps: comparison of recombinant NR1a/NR2A and NR1a/NR2D NMDA receptors. J Physiol 510:1–18.

Xia P, Chen HS, Zhang D, Lipton SA (2010) Memantine preferentially blocks extrasynaptic over synaptic NMDA receptor currents in hippocampal autapses. J Neurosci 30:11246–11250.

Zhang M, Stern JE (2017) Altered NMDA receptor-evoked intracellular Ca (2+) dynamics in magnocellular neurosecretory neurons of hypertensive rats. J Physiol 595:7399–7411.

Zhang SJ, Buchthal B, Lau D, Hayer S, Dick O, Schwaninger M, Veltkamp R, Zou M, Weiss U, Bading H (2011) A signaling cascade of nuclear calcium-CREB-ATF3 activated by synaptic NMDA receptors defines a gene repression module that protects against extrasynaptic NMDA receptor-induced neuronal cell death and ischemic brain damage. J Neurosci 31:4978–4990.

Zhang X, Bai L, Zhang S, Zhou X, Li Y, Bai J (2018) Trx-1 ameliorates learning and memory deficits in MPTP-induced Parkinson's disease model in mice. Free Radic Biol Med 124:380–387.

Zhou M, Zhang W, Chang J, Wang J, Zheng W, Yang Y, Wen P, Li M, Xiao H (2015) Gait analysis in three different 6-hydroxydopamine rat models of Parkinson's disease. Neurosci Lett 584:184–189.

Zhou X, Hollern D, Liao J, Andrechek E, Wang H (2013) NMDA receptor-mediated excitotoxicity depends on the coactivation of synaptic and extrasynaptic receptors. Cell Death Dis 4:e560.